Conversion of human fibroblasts to endothelial-like cells via dedifferentiation to mesodermal progenitors in 3D condensates.

Catherine Jane Pilling

M.Sc. by Research

University of York

Biology

December 2015

Abstract:

We have previously shown that human mesenchymal stromal cells dedifferentiate to early mesoderm when cultured in defined three-dimensional (3D) *in vitro* conditions, to mimic mesenchymal condensation, through a controlled autophagy response. Here it was determined if human dermal fibroblasts (HDFs), a terminally differentiated cell, could similarly undergo dedifferentiation. By varying initiating cell number and culture duration, we identified optimised conditions for HDF dedifferentiation in 3D spheroids. This was revealed by QPCR which identified low level expression of pluripotency factors, Oct4, Sox2 and Nanog, and a 6 to 1200-fold increase in mesodermal markers, Brachyury, Goosecoid and CXCR4, compared to adherent 2D HDFs, whilst expression of the CXCR4 ligand and stromal marker CXCL12 decreased. CXCR4 protein expression was confirmed by western blot analysis and immunostaining, which showed positive distribution across the spheroid. These changes occurred with a concomitant increase in autophagic features (increased TFEB mRNA expression, elevated LAMP-1 protein and the accumulation of autophagosome-like structures). We next tested the redifferentiation potential of 3D HDFs by exposing the disaggregated cells to endothelial growth conditions on Matrigel. When exposed to EGF and FGF-2, endothelial-like networks formed within 7 days, which was reduced to 24h following the addition of IGFI, VEGF and BMP4. These cells were also shown to express low levels of endothelial cell markers, VE-Cadherin, Nrp1, Nrp2 and ALK1 and higher levels of EphB4 and KDR by QPCR. These findings suggest that human cell differentiation can be efficiently reversed by physiological means and then re-differentiated into a new cell type.

List of Contents

List of Tables

List of Figures

Declaration

I declare that this thesis is a presentation of original work and I am the sole author. This work has not previously been presented for an award at this, or any other, University. All experiments were carried out by myself with the exception of the Transmission Electron Microscopy which was prepared and imaged by the technology facility. All sources are acknowledged as references.

1 Introduction

1.1 Introduction to Regenerative Medicine:

The aim of regenerative medicine is to replace or regenerate human cells, tissues or organs to restore the original function. Regenerative medicine by definition covers a wide range of therapeutic approaches spanning from the administration of small molecules to cell based therapies. Since humans only possess a limited capacity to repair and replenish damaged tissues and organs this makes restorative cell therapies mimicking either development or natural examples of regeneration a desirable commodity. During human foetal development highly proliferative multipotent cells progress into an adult phenotype that is no longer capable of regenerating original tissue (van de Ven et al., 2007). Thus adult cell damage is usually 'patched' up using fibroblasts and through the substitution of a cellular matrix resulting in fibrogenesis and the formation of disorganised collagen deposits i.e scar tissue (Gurtner et al., 2008). The resulting fibrosis can be detrimental as evidenced by fibrotic cardiac tissues, which have no regenerative capabilities and is a contributor to heart failure (Chen and Frangogiannis, 2010). Wound repair occurs in the majority of tissues therefore damage due to a myocardial infarction can be compared and is similar to the repair of a burn or spinal-cord injury (Gurtner et al., 2008). Scar tissue usually has less tensile strength and acquires a rigid characteristic meaning that tissues that require integrity, such as skin which acts as a protective barrier, become more fragile (David T Corr, 2009). Tissue damage is a major cause for concern and a main focus for regenerative therapies. Myocardial infarction causes tissue within the heart to become necrotic and the body repairs this through substitution of the necrotic tissue by scar tissue (Ørn et al., 2007). The remaining muscle in the heart is thought to compensate for initial ventricular function (Khan and Sheppard, 2006). However, despite this compensation, the development of scar tissue has been associated with stiffness, hypertrophy and heart failure (Conrad et al., 1995). Therefore one approach has been to develop a cell based therapy in an attempt to restore the missing tissue with *in vitro* grown cardiomyocytes. This aims to avoid the formation of scar tissue and restore the heart back to its original functional state (Ieda et al., 2010; Zhang et al., 2015; Zwi et al., 2009). This and other medical burdens due to the limited repair capacity of adult tissues have prompted researchers to create new therapeutic cell types *in vitro* in order to recapitulate developmental processes that originally created the organ through the use of induced pluripotent stem cells (iPSCs) or partial dedifferentiation.

Other methods could potentially create *in vitro* or *in vivo* situations that mimic to some extent regeneration typically seen in lower organisms such as zebra fish *(Danio rerio)* caudal fin regeneration or newt *(Salamandridae)* lens regeneration. Multiple pathways that are necessary for regeneration in humans are currently being researched in order to discover new potential therapies.

1.2 Tissue regeneration in *vivo*:

There are multiple different examples of organisms that have the potential to partially or fully regenerate organs and whole limbs. Humans generally tend to display poor regenerative ability, with the exception of liver regeneration. In contrast, lower organisms such as salamanders show a much greater regenerative capacity and can fully regenerate many body parts including limb, tail, eye, jaw and the heart (Tanaka, 2003). There are different processes in which different organisms replace damaged or amputated tissues. Human liver is known for its ability to restore itself and allows us to successfully transplant a liver lobe (Botha et al., 2010). Liver regeneration occurs through a pool of adult stem cells known as 'Hering Canal Cell' (Neil D. Theise, 1999). These cells are capable of differentiating via a precursor cell called oval cells into various cell types including hepatocytes and biliary cells to replace and restore damaged tissue (Fausto, 2000; Fausto and Campbell, 2003). This method of regeneration requires a pool of adult stem cells to repair the tissue. However, there is no dedifferentiation or reprogramming necessary. This is one method by which cell therapies could be implemented, but the cells would be differentiated *in vitro* and transplanted to replace the damaged or missing cells. Adult stem cells can be of use in *in vitro* tests in order to create new cell based therapies and bone marrow derived mesenchymal stromal cells (MSCs) in particular have been of great interest (Wei et al., 2013). However, certain adult stem cells are more difficult to harvest than other adult cells and this is frequently due to restricted or inaccessible location and the fact there are such a small number of stem cells (Young and Black, 2004). Specific adult stem cells need to be used for specific injury repair; once again using the example of MSCs they would generally have to be used in bone regeneration or other skeletal tissues into which MSCs differentiate (Wei et al., 2013).

Two main methods of natural regeneration without the use of adult stem cells include dedifferentiation and transdifferentiation. Natural dedifferentiation is when

the cells are reverted back to an earlier form which is still committed to a certain cell type but it regains a capability it lost during the final stages of differentiation such as the ability to proliferate (Jopling et al., 2011). This method of natural dedifferentiation is used by zebra fish as a method to regenerate cardiomyocytes to replace lost ventricular tissue. These fish have been shown to be capable of repairing up to a 20% amputation of the ventricle (Jopling et al., 2010; Poss et al., 2002). When a piece of the ventricle is removed or damaged the remaining fully differentiated cardiomyocytes, with nearly no proliferative capacity, dedifferentiate to a cardiomyocyte precursor cell (Takeuchi, 2014; Zhang et al., 2010). This allows them to proliferate before redifferentiating to regenerate missing tissue (Jopling et al., 2010; Lepilina et al., 2006). This dedifferentiation is thought to occur due to the dedifferentiation of the contractile apparatus and allows it to disassemble to prevent the sarcomere from physically impeding cytokinesis. This means that the cells are capable of dividing and replacing the damaged tissue.

Transdifferentiation is a process that may also lead to the regeneration of lost or damaged tissue. Transdifferentiation occurs when an existing terminally differentiated cell is converted into a different cell type that is required by the organism (Jopling et al., 2011). This differs to natural dedifferentiation as the cell type changes completely as opposed to dedifferentiating to a precursor of the cell type in question and then redifferentiating back to the same cell type. The method of transdifferentation varies between organisms. However, the majority of natural transdifferentiation requires some form of dedifferentiation before the cells can form the required cell type. An example of transdifferentiation occurring in nature is lens regeneration in newts (Maki et al., 2010; Tsonis et al., 2004). When the lens is removed, pigmented epithelial cells (PECs) from the dorsal iris transdifferentiate and regenerate the missing tissue (Tsonis et al., 2004). They are capable of doing this through their ability to dedifferentiate to a point where they can switch their developmental fate. The cells elongate and become columnar and depigmented and genes such as FGF (fibroblast growth factor) and PROX-1 (Prospero homeobox protein-1) that are known to be involved in lens production are also expressed during the regeneration (Tsonis et al., 2004). Once differentiation is reinitiated, specific parts of the aggregate of PECs are capable of forming parts of the lens. Some dedifferentiated PECs induce crystallin synthesis and others create lens fibres and lens epithelium which then continues to proliferate and differentiate to form the lens (Gwon, 2006). This mimics the original lens production during development.

Another example of a natural regeneration process is total limb regeneration in newts which occurs through the formation of a blastema. If the limb is amputated between the shoulder to fingertip area, the wound is quickly coated in epithelial cells to form a wound epidermis (Brockes, 1997). This differs to lens regeneration which is due to plasticity of the pigmented epithelial cells. In contrast during limb regeneration, mesenchymal cells underneath the wound epidermis re-enter the cell cycle and form blastemal cells with proliferating dedifferentiated cells just beneath the apical ectodermal cap (Figure 1.1) (Gilbert, 2000). These cells form what is known as a blastema which is an area from which it is possible to regenerate the limb (Figure 1.1) (Brockes, 1997; Brockes and Kumar, 2002; Tsonis, 1996). Limb blastemal cells will always give rise to a limb due to the fact the cells are usually only capable of differentiating into a local progenitor cell rather than going through a transitional phase as a pluripotent cell (Kim and Stocum, 1986).

These natural occurrences of cell reprogramming have prompted researchers to elucidate the mechanisms by which these organisms regenerate and to attempt to replicate these mechanisms *in vitro* to create potential therapies to treat injuries in human tissues.

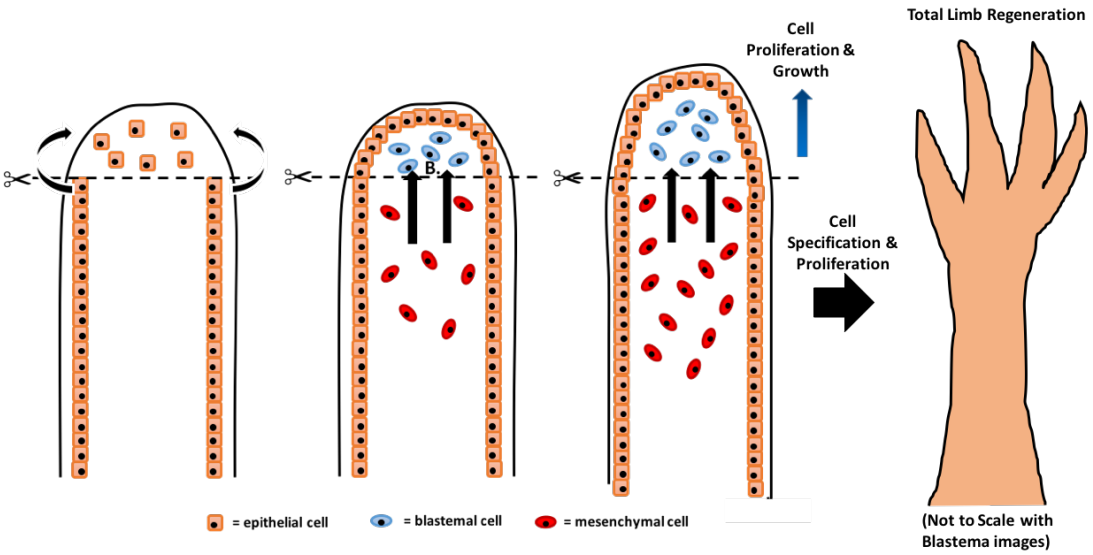

Figure 1.1 Formation of Blastema during Limb Regeneration

The wound is quickly coated in epithelial cells to form the wound epidermis and the mesenchymal cells found in the limb move to the wound and become dedifferentiated blastemal cells to form what is known as the blastema (B). This is then capable of proliferating and reforming the total limb.

1.3 Tissue regeneration *in vitro*:

Regenerative medicine has often focussed on understanding and mimicking developmental processes through the manipulation of adult cells to create new cell types. One main area of research involves inducing dedifferentiation in vitro through various methods, including the introduction of specific factors. A large proportion of potential cell therapies involve the use of induced pluripotent stem cells (iPSCs). iPSCs were generated by the introduction of several important early transcription factors through retroviral tranduction into human dermal fibroblasts. This was initially done using mouse dermal fibroblasts and then using human dermal fibroblasts (Takahashi and Yamanaka, 2006; Takahashi et al., 2007). This method reprogrammes the cells to a pluripotent state through the introduction of factors including a combination of Oct4 (POU5F1), KL4, Sox2 and cMyc or a combination of Oct4, Sox2, Nanog and Lin28 (Takahashi et al., 2007; Yu et al., 2007). These factors had previously been confirmed to be involved in maintaining pluripotency. The creation of iPSCs allows the production of an artificial pluripotent cell type which has the capacity to differentiate into cells from all three germ layers (Hochedlinger and Jaenisch, 2006). *In vitro* differentiation protocols using iPSCs can then be developed to produce the desired cell types. Various differentiation protocols have been described and related to the work presented here, it has been shown that human iPSCs are capable of forming a mixed population of endothelial-like cells (Choi et al., 2009; Kurian et al., 2013). There has even been evidence to suggest that the specific subtypes of endothelial cells, arterial, venous and lymphatic, can be produced (Marcelo et al., 2013). One method of differentiating iPSCs involves using a feeder layer, in this case OP9 feeder. The iPSCS are cultured with the OP9 cells feeders in α-MEM supplemented with 10% FBS and 100μM monothioglycerol (Choi et al., 2009). The cells were shown to express endothelial markers VE-cadherin, KDR and CD31. They were also capable of forming capillary-like networks on Matrigel when grown in the presence of FGF-2 and vascular endothelial cell growth factor (VEGF) (Choi et al., 2009). Further research has shown that it is possible to direct endothelial cell development towards specific subtypes. During vascular remodeling, endothelial cells specialise to acquire the phenotypes and functions to create all three endothelial subtypes (dela Paz and D'Amore, 2009; Podgrabinska et al., 2002). These different subtypes are necessary as arterial cells need to withstand higher blood pressures when compared to venous cells. This preferential differentiation is thought to be achieved through dose-dependent regulation of key differentiation factors VEGF and bone morphogenetic protein 4 (BMP4) (Herzog et

al., 2005; Marcelo et al., 2013). The concentration of VEGF is essential for suppressing or activating a specific endothelial cell phenotype. It is thought that a high concentration of VEGF induces arterial cell differentiation but low to intermediate amounts induce venous specification (Marcelo et al., 2013). Other factors involved such as COUP-TII promote venous differentiation. However, the full mechanism is still not fully understood. The expression of certain factors are used to characterize the specification of endothelial cell subtype. For example EPHB4 and Nrp-2 (Herzog et al., 2005; Marcelo et al., 2013) are expressed by venous endothelium and ALK1, CXCR4, and Nrp-1 (Corti et al., 2011; Herzog et al., 2005; Kurian et al., 2013) are known to be arterial endothelial markers. VE-cadherin is often used as a lymphatic endothelial cell marker (Kurian et al., 2013).

Despite the possibilities of using the iPSCs for producing a desired cell-type, other approaches that do not require forced expression of pluripotency factors are also desirable. This is due to concerns regarding the safety and efficiency of the iPSC process. Research into regenerating tissues *in vivo* has elucidated specific factors and mechanisms necessary for the repair of specific tissues. Earlier dedifferentiation and transdifferentiation *in vivo* were discussed including the examples of cardiomyocyte restoration and newt lens regeneration (Poss et al., 2002; Tsonis et al., 2004). Following the findings in zebra fish concerning cardiomyocyte dedifferentiation and proliferation, this process has been mimicked *in vitro* (Figure 1.2). Now it is possible to induce human cardiomyocytes to undergo senescence withdrawal to allow the cardiomyocytes to proliferate and redifferentiate back into functional cardiomyocytes (Zhang et al., 2010). The ability to produce proliferative cardiomyocytes has an important therapeutic potential as it would give us the ability to restore damaged heart tissue which has restricted repair capability and tend to form scar tissue. Using dedifferentiation in this way usually involves the maintenance of the specific cell type but at an earlier stage. Studies on human cardiomyocytes have shown that it is also possible to induce cardiomyocyte proliferation through the dedifferentiation of the contractile apparatus (Zhang et al., 2010). p38 MAP kinase is known to regulate necessary genes for mitosis in cardiomyocytes such as cyclin A and cyclin B (Ambrosino and Nebreda, 2001; Engel et al., 2005), Adler et al., 2007). Overexpression of p38 MAPK is thought to block cardiomyocyte proliferation and cells with a p38 MAPK inhibitor are shown to undergo higher levels of proliferation. FGF-1 also plays a role as it is known to upregulate genes implicated in regeneration and cell cycle control. Therefore, through the introduction of a p38 MAPK inhibitor combined with FGF-1 stimulation it

is possible to dedifferentiate cardiomyocytes to a stage where they are capable of proliferating (Figure 1.2) (Engel et al., 2005).

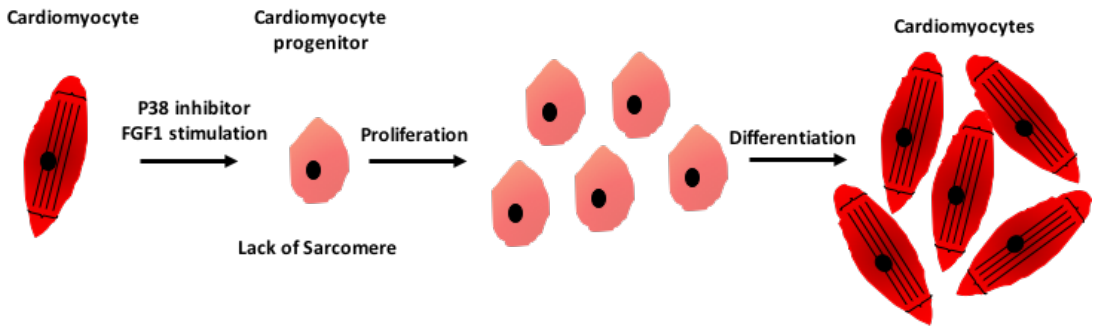

Figure 1.2 Dedifferentiation of Cardiomyocytes to Proliferative Progenitor Cells.

Cardiomyocytes are capable of dedifferentiating to a progenitor cell that is capable of proliferating. This allows the cardiomyocytes that typically do not proliferate to re-enter the cell cycle and divide to replenish damaged or amputated cells.

Recent evidence has shown that it is possible to transdifferentiate cells in a therapeutic manner. An example of this is the transdifferentiation of human dermal fibroblasts to endothelial cells. It was hypothesised that to induce fibroblast to endothelial cell transdifferentiation, endothelial cell specification could be achieved by small molecule activators of toll-like receptor 3 (TLR3) together with micro-environmental conditions (Sayed et al., 2014). The human dermal fibroblasts were grown on gelatin-coated plates and treated with Poly I:C in medium supplemented with serum and a gradually increasing concentration of knockout serum replacement (Figure 1.3) (Sayed et al., 2014). Once the cells had been treated like this for seven days, then the cells were treated with a transdifferentiation medium containing 20ng/ml BMP4, 50ng/ml VEGF and 20ng/ml FGF-2 (Figure 1.3) (Sayed et al., 2014). The transdifferentiated cells were maintained in medium in the presence of FGF-2 and VEGF and 0.1mM 8-bromoadendosine-3': 5'-cyclic monophosphate sodium salt (8-Br-cAMP) which is known to increase endothelial cell specification (Sayed et al., 2014). 78% of cells were shown to express CD31 which is an endothelial cell marker and they also expressed endothelial cell (EC) markers VE-cadherin, KDR, Von Willebrand factor (vWF) and eNOS. Additionally, the cells were tested for their ability to form capillaries on Matrigel (Figure 1.3) which revealed that they were capable of undergoing angiogenesis (Sayed et al., 2014). Other differentiation protocols also

use additional supplements insulin-like growth factor (IGF), cortisol and heparin (Soda et al., 2011). These cells also showed CD31, vWF and KDR expression.

The ability to produce cardiomyocytes and endothelial cells without the use of iPSCs provides promising evidence that environmental cues and specific differentiation factors are enough to cause a change in cell-type.

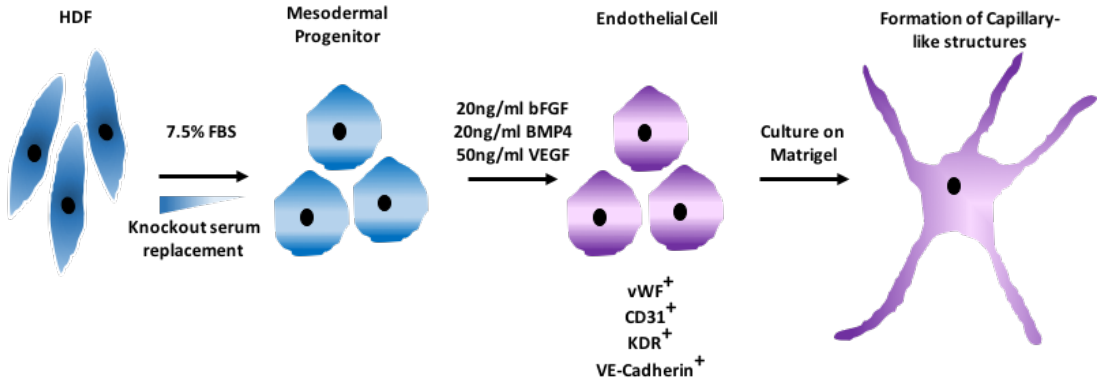

Figure 1.3. Transdifferentiation of HDFs to Endothelial Cells

HDFs have been used in transdifferentiation protocols to create endothelial cells. This is achieved through dedifferentiation to a mesodermal progenitor cell. Then the addition of FGF-2, BMP4 and VEGF to differentiate cells to endothelial cells that express vWF, CD31, KDR and VE-Cadherin.

1.4 Issues involving current *in vitro* methods of reprogramming:

Despite the possible benefits of using iPSCs to create cells for potential transplantation and therapies, the progress of cell therapies using iPSCs depends on the establishment of a safe and efficient method of genetic manipulation. Transduction is a popular route and is usually carried out by the introduction of retroviral vectors (Imamura et al., 2012; Nethercott et al., 2011). Retroviral transduction often involves the use of modified murine leukaemia virus (MLV). The use of viruses is often necessary as the virus DNA forms a large nucleoprotein structure which contains proteins necessary for insertion of viral DNA into the host genome. Hence, despite the method being successful in inducing pluripotency concerns remain about safety and efficacy. Retroviral transduction can be an efficient methods of introducing genes into a host genome. However, retroviral transduction is dependent on a high division rate which varies between cultured cell types and also makes it non-applicable to quiescent cells (Li et al., 2004). A different form of transduction known as lentiviral transduction which involves the use of modified human immunodeficiency virus (HIV) is capable of transducing specific quiescent cells. This means lentiviral transduction is becoming increasingly popular (Naldini et al., 1996; Verhoeyen et al., 2009). A bigger issue with retroviral transduction is the non-specific integration of DNA into the host cell and the number of insertions can vary potentially altering transcription within the cell. It has also been found that the transcription of transduced genes can resume in differentiated iPSCs which could make it dangerous to use virally transduced iPSCs in clinical trials (Okita et al., 2007). This may be problematic for example when the viral DNA integrates and activates nearby oncogenes (Persons, 2010). There have been examples of this in clinical trials of X-SCID disorder that were treated with haematopoietic stem cells transduced with a recombinant retrovirus expressing the common gamma chain of interleukin receptor (Hacein-Bey-Abina et al., 2008). Despite the success that nine out of eleven patients treated had almost fully restored immune systems, four of these nine patients developed T-cell acute lymphoblastic leukaemia between three and six years after treatment. It was confirmed that two of these patients had a copy of the vector DNA found in the first intron of the growth-promoting LM02 gene of the leukaemic clones and upstream of the first exon of the same gene (Hacein-Bey-Abina et al., 2008). LM02 is a LIM domain transcription regulator that is known to be involved in haematopoiesis and is reported to be activated in T cell leukaemia by chromosomal translocation (Yamada et al., 1998). The development of leukaemia was also seen using the same

treatment in a separate clinical trial proving that genes were being integrated into the host (Hacein-Bey-Abina et al., 2003). This illustrates some of the concerns regarding the use of cells that have been altered by retroviral transduction (Hacein-Bey-Abina et al., 2008). Clinical trials using lentiviral transduced cells are being held and safety needs to be further assessed. Additionally, there is also danger of ectopic transcription of Oct4, Sox2, Klf4 and cMyc leading to neoplastic development due to their association with the development of multiple tumours (Ben-David and Benvenisty, 2011).

In addition, there is the concern that pluripotent stem cells are capable of forming teratomas. There have been many different cases where cells that were derived from pluripotent cells have formed teratomas in the host. iPSCs are known to form teratomas when transplanted into mice and therefore have the same adverse potential for the host (Ben-David and Benvenisty, 2011). Therefore this means that a main focus of the ability to use iPSCs in therapies is the requirement to prevent teratoma formation (Lee et al., 2013). However, this hurdle could potentially be avoided by using cell therapies avoiding pluripotency.

1.5 Embryonic Specification During Early Development:

Gastrulation marks the beginning of morphological patterning within the embryo (Ginsburg et al., 1990). This is the stage at which a blastocyst is formed which consists of trophectoderm and the inner cell mass (ICM) (Watson, 1992). Trophectoderm forms a fluid filled cavity and provides the embryo with nutrients and gives rise to the chorionic sac and the foetal component of the placenta and the ICM where the pluripotent progenitor cells are located which develop into each of the three germ layers during gastrulation (Boroviak et al., 2014). The formation of the full embryo and development of the germ layers is thought to be controlled through cell-cell interactions and cell-matrix interactions and also through the expression of specific factors to allow the formation of individual tissues (Figure 1.4) (Poh et al., 2014). Due to the fact that pluripotent factors act to maintain pluripotency therefore preventing differentiation they must be downregulated in a specific manner while the expression of other differentiation-promoting factors is upregulated in order to determine cell fate. Oct4 and Sox2 are closely involved in germ-layer fate specification by enabling cells to integrate signals and thereby determining their fate (Thomson et al., 1998, 2011).

Oct4 has been found to be upregulated in cells committed to a mesendodermal fate but repressed in the neural ectoderm fate (Pan et al., 2002). Sox2 is expressed in neural ectoderm as opposed to mesendoderm (Avilion et al., 2003a). Hence expression levels of these two factors are controlled to allow specific lineages to form. With high Oct4 and low Sox2 mesendoderm is formed. With low Oct4 and high Sox2 neural ectoderm is formed (Avilion et al., 2003b; Nichols et al., 1998; Niwa et al., 2000; Pan et al., 2002). Downregulation of Nanog has also been shown to be a necessary step during lineage specification.

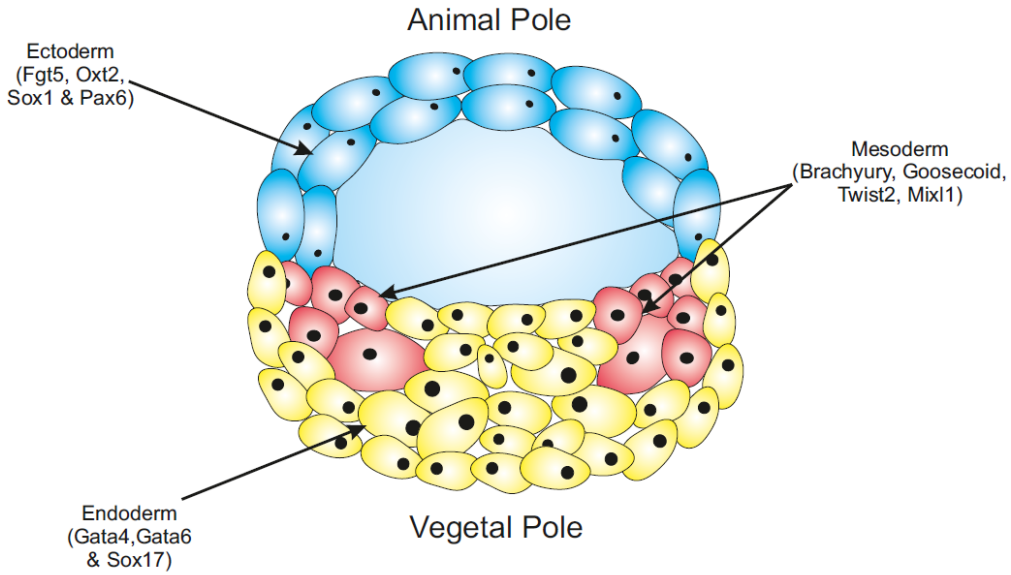

Figure 1.4. Human Blastocyst Structure and Germ Layer Locations.

The gastrulation stage of development is when the three germ layers are starting to form and specific transcription factors used to identify specific germ layers are beginning to be expressed.

The different germ layers are necessary for the formation of different tissues types that will eventually create the embryo. As previously mentioned these three germ layers develop from the ICM. The three germ layers are known as ectoderm, endoderm and mesoderm which can be located in specific locations of the blastocyst during gastrulation (Figure 1.4). Ectoderm generates the outer layer of the embryo and develops into the neural crest, neural tube and surface ectoderm (Correia and Conlon, 2000; Knecht and Bronner-Fraser, 2002; Tadeu et al., 2015).

These develop into the peripheral nervous system, the spinal cord and epidermis to name a few examples of tissues with ectodermal origin (Chang and Hemmati-Brivanlou, 1998). Ectodermal tissues are typically identified through certain markers including Fgf5, Otx2, Sox1 and pax6 (Dimanlig et al., 2001; Okita et al., 2007; Pevny et al., 1998; Rathjen et al., 1999). Endoderm develops into the interior linings of the digestive and respiratory tube (Zorn and Wells, 2009). Thus, endodermal differentiation and patterning leads to the formation of the liver, pancreas and lungs (Kubo et al., 2004; Zorn and Wells, 2009). Endodermal tissues are identified using specific markers such as Gata4, Gata6 and Sox17 (Okita et al., 2007). Endoderm also plays a role in signalling to mesoderm to form muscle in specific formations.

For the purposes of this study the main focus will be on mesodermal lineage specification and mesodermal tissues, specifically endothelium. Mesoderm is first identified during the formation of the primitive streak which then migrates laterally and anteriorly and patterns into populations with specific developmental fates (Lacaud et al., 2004). Mesoderm forms multiple different tissue types including the notochord, skeletal system, muscular system, dermis of skin, kidney, blood, endothelium and cardiovascular tissue (Fehling, 2003; Lacaud et al., 2004; Okita et al., 2007). Mesoderm is known to be directed through controlled decrease in expression of Oct4 but also by specific genes such as Brachyury, Twist2, FoxA2 and Mixl1 (Okita et al., 2007; Poh et al., 2014).As it has been shown that factors such as Brachyury are markers of terminal fate determination towards a mesendodermal commitment. Brachyury has become an important marker of mesodermal specification (Martin and Kimelman, 2010; Smith et al., 1991). These Brachyury-expressing mesodermal progenitor cells are essential to form the different tissues mentioned above including endothelium (Figure 1.5). These cells mature to produce a set of KDR expressing mesodermal progenitor cells which are essential to the formation of the haemangioblast (Figure 1.5) (Choi et al., 1998; Park et al., 2013). The haemangioblast then develops to form haematopoetic cells and endothelium. The haemangioblastic cells that are destined to form endothelium develop into specific endothelial cells to form the vascular and lymphatic system (Figure 1.5) (De Val and Black, 2009). These subtypes of endothelial cells can be identified through specific factors as mentioned in section 1.6. These cells then form the lining of blood vessels and lymphatic vessels which is known as the endothelium (De Val and Black, 2009). This is just one example of the tissues that mesoderm can form, meaning mesodermal progenitor cells could be used in regenerative

medicine to create multiple types of mesodermal tissues *in vitro* for therapeutic purposes.

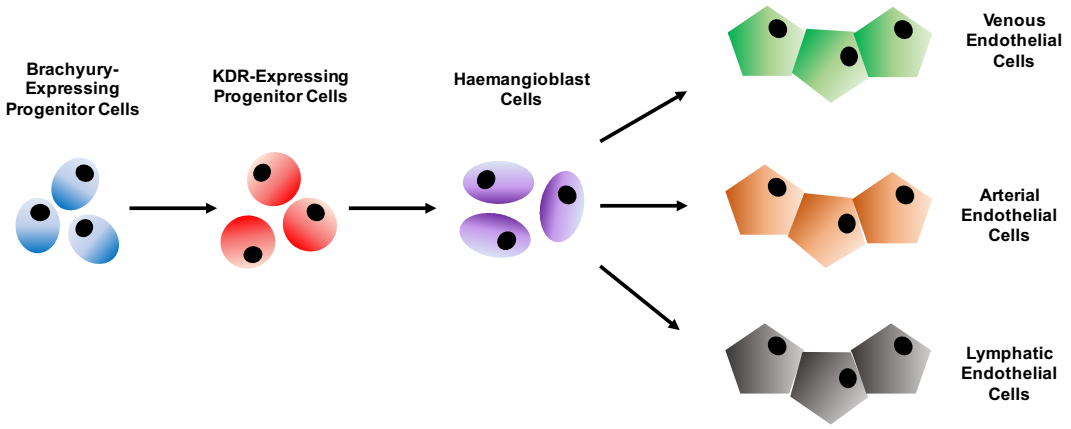

Figure 1.5. Model of Mesodermal Progenitor Cell Differentiation into Endothelial Cells

Development of arterial, venous and lymphatic endothelial cells from a Brachyury-expressing progenitor cells via the formation of the haemangioblast which has endothelial and haematopoietic differentiation potential.

1.6 *In vitro* Differentiation Protocols:

Differentiation protocols have been developed for many years and developmental pathways have been mimicked to produce multiple different cells types such as cardiomyocytes, neural cells and endothelial cells (Wang et al., 2011; Zwi et al., 2009). Many of these protocols initially focussed on the directed differentiation of embryonic stem cells and many different cell types were generated (Bibel et al., 2004; Xu et al., 2002). However, since the development of iPSCs the main focus has shifted more towards the differentiation of iPSCS to generate patient-specific functional cells that could be transplanted to regenerate damaged tissues. An example that is relevant to this project is the differentiation protocol designed to induce endothelial cell differentiation from either embryonic stem cells or iPSCs. Endothelial cells and haematopoietic cells are thought to develop from the same precursor cell known as the the haemangioblast. It is thought that the haemangioblast develops into an endothelial progenitor cell that is capable of differentiating into an endothelial cell or a haematopoietic cell (Fehling, 2003; Xiong, 2008). Endothelial cells form an important lining of the entire vascular system known

as the endothelium (Lerman and Zeiher, 2005). The endothelium is a semi permeable membrane and controls the transfer of small and large molecules. Both endothelial cells and the endothelium are involved in multiple biological functions. Examples of these functions include thrombosis and thrombolysis, which is the creation and break down of blood clots, and platelet adherence and regulation of vascular tone and blood flow (Verhamme and Hoylaerts, 2006). Finally, the endothelium is also involved in the regulation of leukocyte, monocyte and lymphocyte interactions with the vessel wall which control immune responses specifically inflammation (Danese et al., 2007). There are also associated pathologies linked to endothelial cells that have discordant stimulation or a lack of control of endothelial cell response. These conditions include atherosclerosis, vasculopathy, hypertension, congestive heart failure and inflammatory syndromes (Rajendran et al., 2013), which are related to endothelial injury and dysfunction.

The majority of endothelial differentiation protocols using pluripotent cells initially include a step to create a mesodermal progenitor cell which is usually achieved by exposure to specific growth conditions. An example of such conditions is growth of iPSCs in a mesodermal induction medium which consists of DMEM:F12 with 15mg/ml stem cell grade bovine serum albumin (BSA), 17.5µg/ml human insulin, 275µg/ml human holo-transferrin, 20ng/ml FGF-2, 50ng/ml human VEGF-165, 25ng/ml human BMP4, 450 monothioglycerol and 2.25mM each L-glutamine and non-essential amino acids (Kurian et al., 2013). There are multiple markers that have been found in early endothelial progenitor cells/angioblast cells including KDR and CD133 (Asahara et al., 1997). These are cells are derived from the haemangioblast but have differentiated to an early endothelial progenitor cell. When these cells then start to develop they lose CD133 when differentiating into more mature endothelial cells and they gain VE-cadherin and von Willebrand factor. In the study by Kurian *et al*, after 8 days there was a peak in the $CD45^{+}$ cell population with an increase in CD31 and mesodermal progenitor markers and downregulation of pluripotency-related factors (Kurian et al., 2013). It is thought that these cells could be representative of a developmental stage similar to the angioblast. The cells were tested for their ability to differentiate into an endothelial-like cell and they showed upregulation of endothelial markers VE-cadherin, vWF and KDR. This process using iPSCS takes approximately 24 days (Kurian et al., 2013). The endothelial cells were tested for markers specific to certain subtypes of endothelial cell. These included eight arterial markers ALK1, Nrp-1, CXCR4 and EPHB2, three venous markers COUP-TFII, EPHB4 and Nrp-2 and 4 lymphatic/pan endothelial markers PROX2,

VEGFR3, vWF and CDH5. Increased expression of these markers was shown (Kurian et al., 2013). The cells were also tested for their functionality by testing their ability to form capillary like structures when grown on Matrigel and their ac-LDL uptake (Kurian et al., 2013).

There are variations between different differentiation media. The basic combination that the majority of differentiation media contain includes the use of the supplements vascular endothelial growth factor (VEGF) and bone morphogenetic protein-4 (BMP4) which is added to Minimum Eagle's Medium along with the basic cell growth supplements: 20% FBS, L-glutamine, beta-mercaptoethanol and 1% non-essential amino acids (Kurian et al., 2013; Sayed et al., 2014). There are other media that contain other factors such as insulin-like growth factor and TGF-beta which are also thought to aid endothelial cell differentiation (Marcelo et al., 2013). However, the essential factors that appear in most differentiation protocols are VEGF at approximately 50ng/ml, FGF-2 at approximately 20ng/ml and BMP4 where the concentration varies considerably between different protocols (Breier et al., 1992).

1.7 Using a 3D in vitro culture model system to dedifferentiate Mesenchymal Stromal Cells (MSCs):

Previous work in this laboratory has shown that bone marrow-derived mesenchymal stromal cells (MSCs) undergo dedifferentiation to an early mesendoderm-like state when grown as 3D spheroids in non adherent 96-well U-bottomed plates in 0.25% methyl cellulose in DMEM for five days at 37°C and 5% CO_2 (Figure 1.6). It was proposed that this model of dedifferentiation has very broad similarities to the formation of a blastema; the condensate of mesenchymal cells from which the regenerated tissues can arise and in lower organisms can enable whole limb regeneration (Tsonis, 1996). Using 3D culture it was shown that 3D MSCs have low level mRNA expression of the pluripotency factors Oct4, Sox2 and Nanog (Pennock et al., 2015). When the levels were compared to embryonic stem cells they were considerably lower (Pennock et al., 2015a). In contrast, 3D MSCs expressed high levels of CXCR4, Brachyury, Goosecoid Mixl and KDR mRNA with widespread protein expression of CXCR4, Brachyury and KDR. (Pennock et al., 2015). These data show that the cells cultured in 3D are not pluripotent but may be at an equivalent developmental stage to early mesoderm based on marker expression. Additionally, CXCR4 has been shown to mediate homing of specific stem cells

during development, such as haematopoietic stem cells which also develop from a mesodermal lineage (Miller et al., 2008; Smith et al., 1991). Expression of both Brachyury, Goosecoid and CXCR4 increases with initial differentiation into definitive mesoderm but then starts decreasing when the cells begin to mature further (Miller et al., 2008; Rettig et al., 2012; Takenaga et al., 2007).

This previous work led to the proposal that the 3D-induced dedifferentiation phenomenon occurred at least in part through a controlled autophagy response. Autophagy is the mechanism by which cells survive under stress by removing damaged cellular contents such as mitochondria, ER and misfolded proteins (Glick et al., 2010). By exposing the cells to 3D culture it is possible to optimise the process of clearing damage from the cells and enable rejuvenation and dedifferentiation. This was seen by mRNA expression of TFEB and upregulated protein expression of LAMP-1 (Pennock et al., 2015). Transmission Electron Microscopy (TEMs) showed increased autophagosome- and lysosomal-like structures which also points towards an increase in autophagy (Pennock et al., 2015). In addition, it was demonstrated that during dedifferentiation in 3D, the cells switched from oxidative phosphorylation to anaerobic-type metabolism. This type of metabolic switch has been confirmed to occur in cells dedifferentiating towards pluripotency (Folmes et al., 2011; Varum et al., 2011). Blastemal cells have also been reported to switch to glycolytic metabolism (Gilbert, 2000; Tsonis, 1996; Varga et al., 2014)

3D MSCs that were transplanted into mice remained small and generated highly organised defined mesodermal structures including muscle, cartilage and connective tissue (Pennock et al., 2015). The benefits of producing a cell that is not fully reprogrammed to a pluripotent state (unlike iPSCs) means they do not form teratomas. When placed in mice tissue they appear only to be capable of forming tissues of mesodermal origin (Pennock et al., 2015). This method is efficient, synchronous and could potentially be adapted for cell types, such as fibroblasts which are often the cell of choice in iPSC reprogramming. The ability to dedifferentiate cells through modifying their growth environments also avoids the concerns involving retro-/ lentiviral transduction which were mentioned previously.

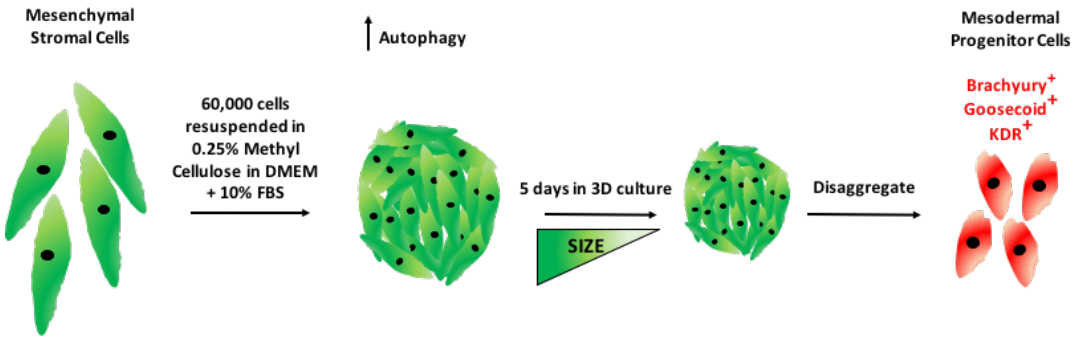

Figure 1.6. Dedifferentiation of Mesenchymal Stromal Cells in 3D Culture.

Bone marrow mesenchymal stromal cells (MSCs) undergo dedifferentiation to an early mesendoderm-like state when grown as 3D spheroid cultures in a size- and time-dependent manner. MSCs are grown in 96-well U-bottomed plates in 0.25% methyl cellulose in DMEM for five days at 37°C and 5% CO_2.

1.8 Project Aims

It was hypothesised that adult human dermal fibroblasts (HDFs) can be dedifferentiated using specific 3D culture conditions and the dedifferentiated HDFs can be directly reprogrammed into endothelial-like cells.

The aims of this project are:

1. Determine whether adult HDFs dedifferentiate to an early mesoderm-like state when cultured in 3D conditions.
2. Investigate whether autophagy has a role in the dedifferentiation process.
3. Investigate the capacity of the dedifferentiated HDFs to convert to endothelial-like cells using defined (re)differentiation protocols.

2 Methods

2.1 Cell Culture

2.1.1 HDF Expansion Conditions:

Adult HDFs were cultured in Dulbecco's Modified Eagle Medium (DMEM) supplemented with 10% foetal bovine serum (FBS) and 1% penicillin and streptomycin (P/S) at 37°C in 5% CO_2 atmosphere. DMEM and P/S were supplied by Invitrogen and FBS by Biowhittaker. HDFs were trypsinised in 1x trypsin and passaged at a ratio of 1:2- 1:4 and then placed into the necessary number of flasks. HDFs used experimentally were at a variety of Passages (9-20) and were supplied by Fischer Scientific (Cat. No. 10407693 & unknown).

2.1.2 HUVEC expansion conditions:

HUVECs (PromoCell GmbH) were cultured in Endothelial Cell Growth Medium 1 (PromoCell, Cat. No. C-22010) with the endothelial cell growth supplements provided at 37°C in 5% CO_2 atmosphere. Flasks were coated with gelatin by adding sterile water with 0.1% gelatin for five minutes. Then the excess water was removed and the flasks were left to dry for one hour in a class II safety cabinet. HUVECs were trypsinised in 1x trypsin and passaged at a ratio of 1:2-1:4. The cells were then placed into the necessary number of gelatin coated flasks. HUVECs used experimentally were at Passages 5-12.

2.1.3 HDF 3D culture conditions:

Just prior to confluency HDFs were trypsinised, counted using a haemocytometer and centrifuged at 400xg for five minutes. The cells were then resuspended in the correct amount of 3D culture media as described in 2.1.1. with the addition of 0.25% methyl cellulose in order to increase spheroid stability. The cells were placed in a 96-well round bottomed plates and left to incubate at 37°C with 5% CO_2. The spheroids were split-fed by removing two-thirds of the 3D media and replacing it with fresh 3D media.

2.1.4 3D HDF snap freezing and sectioning:

HDF spheroids were removed from the 96-well round bottomed plates and placed into an Eppendorf lid. O.C.T mounting medium was added and the sample was frozen in liquid nitrogen. Then using a Bright's cryostat, 10µm sections were cut and collected on slides in preparation for immunostaining.

2.2 RNA Extraction and Processing

2.2.1 Cell Lysis:

Cells were suspended in 1x PBS and centrifuged at 400xg for 5 minutes. RNA was then extracted using the Nucleospin Kit by Machinery-Nagel, according to the manufacturer's instructions and using the buffers provided. The cells were then resuspended in 350µl cell lysis buffer RA1, containing 3.5µl beta-mercaptoethanol (Sigma, Cat. No. M6250), and pipetted gently. The lysate was filtrated through the NucleoSpin Filter.

2.2.2 RNA extraction:

Once the cells were lysed and filtered, the RNA was extracted following the protocol from Macherey-Nagel using the buffers provided. 350µl of 70% ethanol was added to the filtrate and mixed. The mixture containing the RNA was centrifuged through an NucleoSpin RNA Column at 11,000xg for one minute in order to bind the RNA. A pre-DNAse digestion step included desalting the silica membrane. This was done by adding 350µl Membrane Desalting Buffer (MBD) to the column and centrifuging at 11,000xg for one minute. The DNA was digested using 10µl reconstituted rDNase diluted in 90µl Reaction Buffer for rDNase. The rDNase was added and incubated at room temperature for 15 minutes. The silica membrane was then washed using buffer RA2 in order to inactivate the rDNase. The membrane was washed twice more using buffer RA3. The column was then centrifuged at 11,000xg for one minute in order to assure the membrane no longer contained any RA3 buffer. 30 µl RNase-free H_2O provided was added to the column and centrifuged at 11,000xg for one minute into a clean collection tube to elute the bound RNA. This was done to elute

the bound RNA. The RNase-free H2O was run through the column twice in order to ensure elution of all the bound RNA.

2.2.3 CDNA synthesis:

Using the RNA extracted using the Nucleospin RNA Kit, cDNA was synthesised using Oligo dT kit (Invitrogen, Cat. No. 18418-012) for PCR. RNA was mixed with 1µl of Oligo dt primer, 1µl of 10mM dNTPs and made up to 12µl using H_2O. Samples were mixed using a picofuge then incubated at 65ºC for five minutes, and then chilled for two minutes and microfuged to collect the contents. 7µl of a master mix (4µl 1^{st} Strand buffer, 2 µl 0.1M DTT and 1µl H2O) was added to the sample and incubated at 42ºC for two minutes. 1µl of Superscript II was added to samples with the exception of a control without reverse transcriptase. Samples were mixed and incubated at 42ºC for one hour in order to have the reverse transcriptase at optimal conditions. The reverse transcriptase was then inactivated by incubating the sample at 70ºC for 15 minutes.

2.2.4 Quantitative real-time PCR:

The cDNA was used for quantitative real-time PCR (QPCR) in 96-well plates. Each well contained 17µl of a master mix, which consisted of 10µl SybrGreen (Applied Biosystems, Cat. No. 10459604), 5.5µl H2O and 1.5µl primer of interest (50% forward, 50% reverse). 3µl of cDNA was then added to each well and the plate was centrifuged. The QPCR plate was then read using StepOnePlus Real Time PCR System. The general housekeeping gene used for all QPCR done was GAPDH (Table 1). Controls for all QPCR include testing each mastermix with 3µl of H_2O and the no-reverse transcriptase control in GAPDH mastermix. Primers for VE-Cadherin, Nrp-1, Nrp-2, ALK1 and EPHB4 sequences were published previously (Table 1) (Kurian et al., 2013).

Gene	Forward Primer Sequence (5'-3')	Reverse Primer Sequence (3'-5')	GenBank Ac. No. or Paper
GAPDH	TGCACCACCAACTGCTTAGC	GGCATGGACTGTGGTCATGAG	NM_002046
Oct4	CCCACACTGCAGATCAG	GGGTGTGACGTCTAGTC	NM_002701
Sox2	GAGAACCCCAAGATGCACAAC	CGCTTAGCCTCGTCGATGA	NM_003106
Nanog	CCTCCATGGATCTGCTTATTCAG	CGCTTAGCCTCGTCGATGA	NM_024865
Brachyury	GGGTCCACAGCGCARGAT	TGATAAGCAGTCACCGCTATG	NM_003181
Goosecoid	GATGCTGCCCTACATGAACGT	CTACGACGGGATGTACTTG	NM_173849
CXCR4	CGCCTGTTGGCTGCCTTA	ACCCTTGCTTGATGATTTCCA	NM_003467
CXCL12	CCGTCAGCCTGAGCTACAGAT	GGCAGTCGGACTCGATGTCTA	NM_001008540.1
TFEB	CCAGAAGCGAGAGCTCACAGAT	TGTGATTGTCTTTCTTCTGCCG	NM_007162
KDR	TGATGCCAGCAAATGGGAAT	CCACGCGCCAAGAGGCTTA	NM_002253
VE-Cadherin	GACCGGGAGAATATCTCAGAGT	CATTGAACAACCGATGCGTGA	Kurian et al. 2013
Nrp-1	ACCCAAGTGAAAAATGCGAATG	CCTCCAAATCGAAGTGAGGGTT	Kurian et al. 2013
Nrp-2	AACTGCGAGTGGATTGTTTACG	TCTCGATTTCAAAGTGAGGGTTG	Kurian et al. 2013
EphB4	CCACCGGGAAGGTGAATGTC	CTGGGCGCACTTTTTGTAGAA	Kurian et al. 2013
ALK1	CGAGGGATGAACAGTCCTGG	GTCATGTCTGAGGCGATGAAG	Kurian et al. 2013

Table 2.1. QPCR Primers used for QPCR analysis of 3D HDFs.

2.3 Protein-based analyses

2.3.1 Protein Extraction:

Samples were prepared either through trypsinisation or disaggregation and washed twice in 1x PBS. The samples were then resuspended in RIPA buffer (Thermo Scientific) containing 0.5% protease inhibitor cocktail set III (Calbiochem) and 100μM Na_3VO_4 (Sigma). The sample was then frozen at -80ºC until needed. The samples were centrifuged at 14,000xg for 10 minutes at 4ºC to separate the insoluble fraction from the sample. Supernatant containing the soluble fraction was then transferred to a fresh Eppendorf. Protein quantification was performed using the BCA protein Assay Kit (Thermo Scientific). The protein concentrations were calculated from a standard curve generated from standard samples of known concentration using absorbance measurements at 570nm.

2.3.2 Western Blot Analysis:

Protein samples were prepared for western blotting by mixing samples of 20μg/well protein quantity 3:1 with 4X loading buffer and heated to 95°C for 5 minutes. Samples were loaded into a 10% acrylamide gel and electrophoresed at 130V for 90 minutes. Proteins were then wet-transferred onto a nitrocellulose membrane. Primary antibodies against LAMP-1 and CXCR4 (Table 2) were diluted in Tris-Buffered Saline and Tween20 (TBS-T) plus 4% Marvel and left to incubate in a heat sealed bag whilst rotating overnight at 4°C. Following washing in TBS-T HRP-labelled (horse radish peroxidase) secondary antibodies were added and left to incubate for one hour at room temperature. Membranes were prepared for imaging using Enhanced ChemiLuminescence (ECL) reagents (Promega) following the manufacturer's instructions and images were taken using the Genescan software and Geldoc system.

Antibody	Host	Dilution (Western blot)	Supplier	Cat. No.
CXCR4	Rabbit	1:1000	Millipore	AB1846
LAMP-1	Mouse	1:1000	Developmental Studies Hybridoma Bank	H4A3
Anti-CXCR4	Goat	1:400	Sigma	unknown
Anti-Mouse IgG (HRP Conjugate)	Goat	1:2000	Santa Cruz Biotechnology	sc-2005
Anti-Rabbit IgG (HRP Conjugate)	Swine	1:2000	Dako	P0399

Table 2.2. List of Antibodies Used for Western Blotting and Immunostaining

2.4 Immunocytochemistry:

Spheroids were sectioned (see section 2.1.4.) and then fixed using 4% paraformaldehyde for 10mins at room temperature. The sections were then washed using 1x PBS and blocked with a blocking buffer (1x PBS and 10% sheep serum). The blocking buffer was drained off and the sections were incubated with Anti-CXCR4 (1:100 dilution) overnight at 4°C in a humidified container. Samples were washed three times for 5 minutes in 1x PBS then incubated with sheep anti-rabbit IgG-Cy3 (1:400 dilution) for 1 hour. The washing step was repeated and the samples were mounted using Vectashield mounting medium containing DAPI and imaged by confocal microscopy. Controls included an isotype control, where non-immune rabbit IgG was used in the place of the anti-CXCR4 and a PBS-control where only the secondary antibody was added.

2.5 Transmission Electron Microscopy (TEM):

2D and 3D HDFs were collected in Eppendorf tubes and prepared for TEM by the Biology Technology Facility. They were fixed in 8% formaldehyde, 5% glutaraldehyde in 100mM phosphate buffer mixed 50/50 with 3D HDF medium for 10 minutes followed by fixing with 4% formaldehyde, 2.5% glutaraldehyde in 100mM phosphate buffer, pH7.2 for 30 minutes at room temperature. Samples were then washed in 100mM phosphate buffer, 2 x 20 minutes. Once fixation was complete, the samples were chilled on ice for 60 minutes in 1% OsO4 in 100mM and then washed in 100mM phosphate buffer for 2 x 10 minutes. The sample was then dehydrated in 25%, 50%, 70%, and 90% ethanol for 20 minutes, respectively with a final incubation in 100% ethanol 2 x 20 minutes at room temperature. The sample was then incubated in epoxy propane for 15 minutes. Finally, the sample was incubated 3 times for 30 minutes in 3 different ratios of epon araldite to epoxy propane at room temperature. (25% epon araldite & 75% epoxy propane, 50% epon araldite & 50 % epoxy propane, 75% epon araldite & 25% epoxy propane) with one final incubation in 100% epon araldite before the samples are ready to be sectioned. Polymerised sample blocks were then sectioned at 70nm using a Leica RM2165 rotary microtome and imaged on a FEI Tecnai G transmission electron microscope.

2.6 Disaggregation of spheroids:

The spheroids were removed from the 96-well plate and centrifuged at 1200rpm for five minutes at 4ºC to remove the 3D culture media. The spheroids were washed in 5ml 1x PBS and centrifuged. The spheroids were then resuspended in 1x trypsin and incubated at 37 ºC for five minutes and disaggregated by gently pipetting for no longer than 15 minutes. Serum-containing cell culture was added to deactivate the trypsin and the cells collected by centrifugation.

2.7 Network-forming Assay:

The network-forming assay was performed using Matrigel (Corning, Product Number 354234) and endothelial cell growth media (PromoCell). Matrigel was thawed on ice to prevent it from prematurely polymerising. Once the Matrigel had thawed it was diluted using an equal amount of endothelial cell media and then 200

µl of the mix was added to the individual wells of a 24-well tissue culture plate, making sure the gel was evenly distributed. The plate was then incubated at 37 ºC for 30 minutes to allow polymerisation. Cells were disaggregated (see section 2.6) and washed in serum-containing medium then resuspended at 500,000 cell/ml in complete endothelial cell growth media (EGM) 1-2 (Promocell, Cat. No. C-22010 & C-22011) and EGM 3-5 are made up of EGM2 with either VEGF (R & D Systems, Cat. No. 293-VE), BMP4 (Peprotech, Cat. No. 120-05-5) or a combination of both. Each culture well had 1ml of cell suspension added to it and was incubated at 37 ºC in 5% CO_2. Network-images were taken using a Leica DC 500 microscope using the LCM and brightfield filters.

Supplements	**EGM1**	**EGM2**	**EGM2 + VEGF**	**EGM2 + BMP4**	**EGM2 + BMP4 & VEGF**
Fetal Calf Serum	0.02ml/ml	0.02ml/ml	0.02ml/ml	0.02ml/ml	0.02ml/ml
EGM Suppl.	0.004ml/ml				
EGF	0.1ng/ml	5ng/ml	5ng/ml	5ng/ml	5ng/ml
FGF-2	1ng/ml	10ng/ml	10ng/ml	10ng/ml	10ng/ml
IGF-165		20ng/ml	20ng/ml	20ng/ml	20ng/ml
VEGF-165		0.5ng/ml	50ng/ml	0.5ng/ml	50ng/ml
Ascorbic Acid		1µg/ml	1µg/ml	1µg/ml	1µg/ml
Heparin	90µg/ml	22.5µg/ml	22.5µg/ml	22.5µg/ml	22.5µg/ml
Hydrocortisone	1µg/ml	0.2µg/ml	0.2µg/ml	0.2µg/ml	0.2µg/ml
BMP4				5ng/ml	5ng/ml

Table 2.3. List of Endothelial Cell Growth Medias Used for Network-forming Assay

2.8 Rhodamine-Phalloidin Staining:

HDFs were washed in 1% PBS and then fixed using 4% paraformaldehyde for 10 minutes. HDFs were permeabilized with 0.15% Triton X-100 for 30 minutes before adding rhodamine-phalloidin (ThermoFisher, Cat. No. A22287) at a dilution of 1:1000 and incubated for 1.5 hours in the dark to label the actin cytoskeleton. HDFs were then washed using 1x PBS and the cells were imaged in the cell culture well and viewed using a multiphoton microscope (Zeiss LSM 780).

2.9 AcLDL Uptake:

3D HDFs were disaggregated (see section 2.6) and grown on Matrigel in EGM 1 as described in section 2.7. Once the cells had formed networks acLDL uptake was observed using 50µl of Dil-acLDL (Biomedical Technologies Inc, Cat. No. BT-902) was added to 200µl of EC Media 1 and incubated at 37 ºC in 5% CO_2 for five hours. The cells were then washed in 1ml of 1X PBS three times and imaged using a confocal microscope (Zeiss LSM 710).

3 Results

3.1 Spheroid Condensation:

Mechanical stimuli and cell interactions have been shown to be essential for the development of a fully formed embryo. There are multiple examples of mechanical stimuli that play a role in cell lineage commitment during the development of certain tissues. A few examples of mechanical stimuli and its effects are osmotic pressure altering egg cells as they travel to the uterus or shear stress such as the heart pumping blood which plays a role in endothelial cell and haematopoietic cell fate determination (Horner and Wolfner, 2008; Mammoto and Ingber, 2010; North et al., 2009). Alternatively spheroid-like structures have been seen in other natural processes such as in the formation of the blastema. The blastema is found in embryonic development and during limb regeneration in lower organisms. This suggests that cell aggregation and mechanical stimulation are important processes for development and regeneration and possibly dedifferentiation.

In previous experiments MSCs were shown to condense when grown in 3D *in vitro* culture conditions, which was thought to be mimicking the developmental stage where MSCs form a cell condensate. This is a very early and critical stage during the formation of various organs including cartilage, bone, muscle and more. The cells gather in order to differentiate into different cell types. There are many factors that control mesenchymal condensation formation including changes in cell proliferation and reorganisation of the extracellular matrix (Frenz et al., 1989). The mechanism in which mesenchymal condensation controls cell fate has not been fully elucidated. However, because mechanical stimuli are known to play a role in development and cell specification, it suggests that the mechanical forces created during mesenchymal condensation could be playing a role in differentiation and cell fate determination. Alternatively, the formation of this mass of cells could be mimicking the blastemal characteristics as the results that show broad similarities between the 3D culture system and blastema formation.

Using the same growth conditions as those used to generate 3D MSCs (section 2.1.3.) it was determined whether HDFs similarly underwent 3D-induced condensation.

Spheroids containing 30,000 HDFs and 60,000 HDFs were made and the size change was monitored over five days (section 2.1.3.). Brightfield images of

spheroids were taken on days one to five to monitor size change over time. Images show that there is a visual size decrease and the main size change can be seen between days one to three (Figure 3.1a). The spheroids were measured using ImageJ and a graph was plotted of the size change in μm (Figure 3.1b). The largest size change of 190μm was measured between days one to three. Once day three of 3D culture was reached, the size appeared to be maintained or decreased very slightly. In order to visualise this pattern, a graph of the percentage change was also plotted (Figure 3.1c). The graph of the percentage change shows a steep reduction in size between days one to three and then a clear plateau at day three for both 30,000 and 60,000 spheroids. The 60,000 HDF spheroids show a clear plateau in respect to size change and the size measured at day three is maintained on the following days whereas the 30,000 HDF spheroids continued to condense and decrease in size at a much slower rate. This suggests that the HDFs are also condensing to form these 3D aggregates or blastemal-like structures similar to the MSCs that were grown in 3D culture (Pennock et al., 2015).

Additionally, spheroids were sectioned and stained with toluidene blue and imaged in order to determine changes in the internal organisation of the spheroid (Figure 3.2a). The micrographs show that there is a fairly even distribution of cells throughout the spheroid. However, there also appears to be a slightly more cell dense area towards the centre of the spheroid with fewer cells towards the outside of the 3D structure (Figure 3.2b and 3.2c).

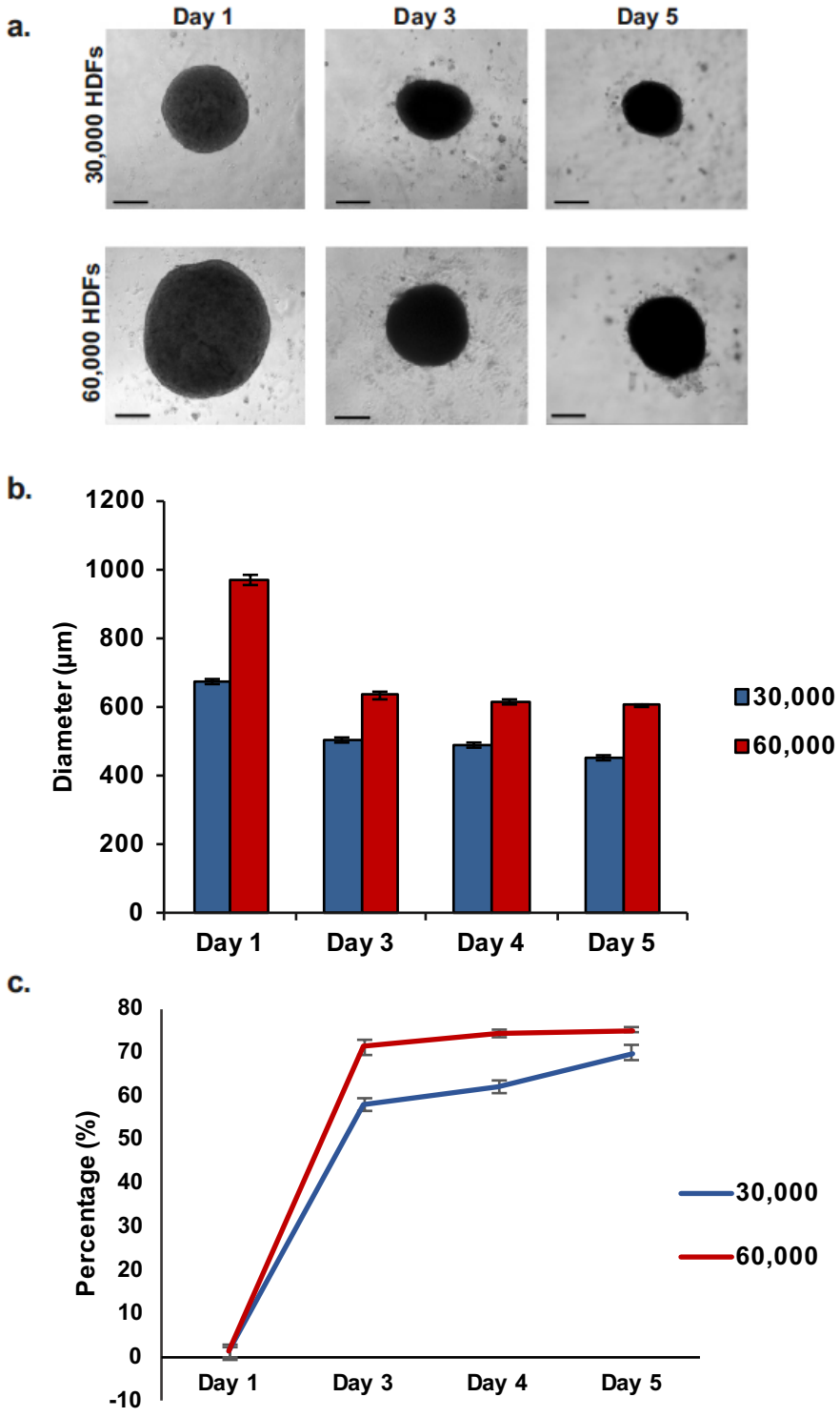

Figure 3.1. Condensation of HDF Spheroids in 3D *in vitro* Culture Conditions.

Decrease in diameter of the HDFs when cultured in 3D. a) Brightfield images of the spheroids (sizes 30,000 and 60,000) from which diameters were measured. b) Graph of the mean size decrease (µm) of six spheroids over a five day period ± SEM. c) Graph of the percentage size shrinkage over five day period.

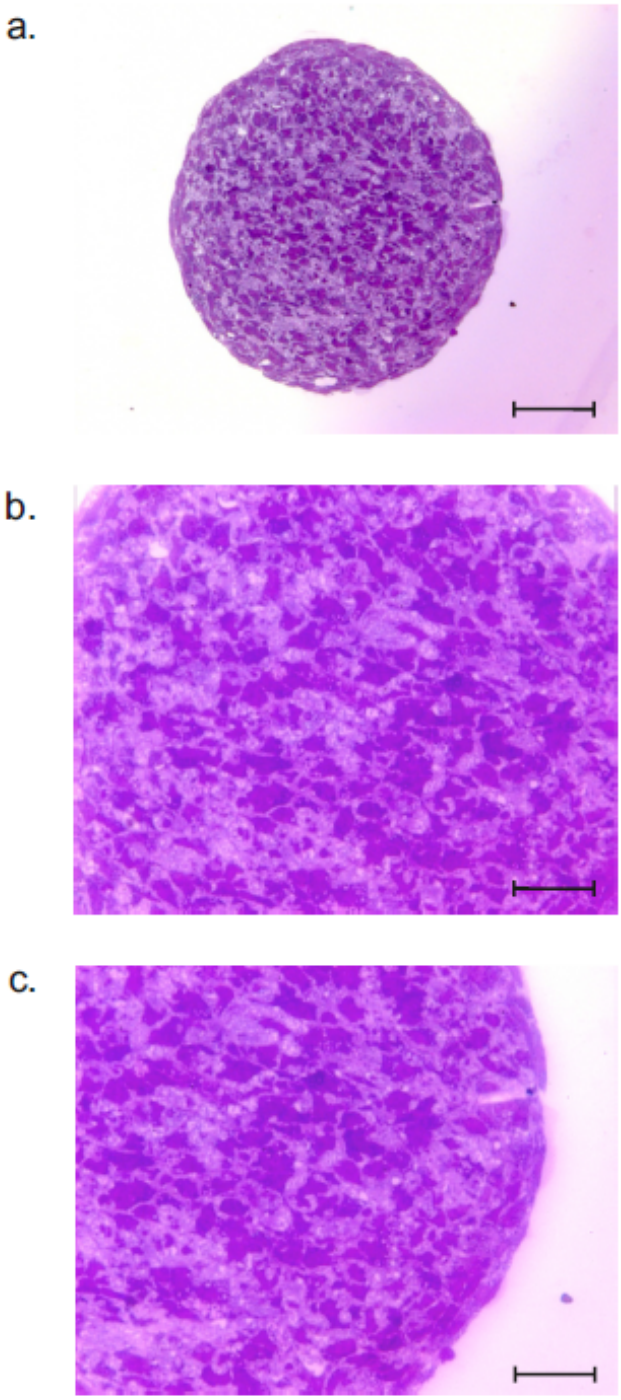

Figure 3.2. Toluidene Blue Staining of 3D HDF Spheroid Sections.

HDFs were grown as 30,000 HDF spheroids for four days fixed and sectioned (see sections 2.1.3. & 2.5) then stained with toluidene blue. a) Whole section image (scale bar = 100μm). b) Centre of the spheroid (scale bar = 50μm). c) Edge of spheroid (scale bar = 50μm)

3.2 Determining the Optimal Spheroid Size and Culture Time:

The HDFs were initially tested to determine whether they would also dedifferentiate in 3D growth conditions, similar to that of 3D MSCs. This was confirmed through QPCR of pluripotency factors Oct4, Sox2 and Nanog. All three of these factors are absent from fully differentiated adult cells meaning upregulated expression would suggest dedifferentiation is occurring (Masui et al., 2007).

3D HDFS from two different donors were grown as 30,000 and 60,000 HDF spheroids and cultured for up to five days (see section 2.1.3.). The highest size and time-dependent increase in expression of pluripotency factors was used in order to decide the optimal 3D culture conditions for HDFs. RNA was extracted from spheroids on days three to five and processed using methods described in section 2.2. The expression of Sox2, Oct4, Nanog was determined using QPCR (Figure 3.3). Oct4 expression levels increased in both the 30,000 and 60,000 HDF spheroid sizes over the five day 3D culture period. By day three the expression levels had increased 6-fold for 30,000 HDF spheroids and 12-fold for 60,000 spheroids. Both spheroid sizes maintained higher but varying expression levels of Oct4 than the HDFs grown in standard 2D monolayer conditions (Figure 3.3a). The 60,000 HDF spheroids increased to approximately 16-fold by day five. However, the highest fold change was seen in the 30,000 HDF spheroids at day four with an 18-fold increase in Oct4 expression (Figure 3.3a). The same samples were also tested for Sox2 expression. Similarly, to Oct4 expression both the 30,000 and 60,000 HDF spheroids had increased Sox2 expression by day three, with much higher fold changes (13-fold increase and a 27-fold increase, respectively) compared to Oct4 (Figure 3.3b). The expression levels of Sox2 for both spheroid sizes varied but also remained higher than HDFs grown in standard 2D conditions throughout the time in culture. Once again the highest fold-change was seen on day four in the 30,000 HDF spheroids with a fold change of approximately 42, whereas the highest fold change for the 60,000 HDF spheroids was the day three 27-fold change (Figure 3.3b). Finally, Nanog expression also increased in 3D culture by day three to a 9-fold increase in 30,000 HDF spheroids and 11-fold increase in 60,000 HDF spheroids and despite variation also remained above the 2D HDF expression levels (Figure 3.3c). The largest fold change was a 24-fold change observed in 30,000 HDF spheroids on day four similar to the expression levels of Oct4 and Sox2 and a 25-fold increase in 60,000 HDF spheroids on day five (Figure 3.3c). From these data, the optimal size and time for dedifferentiation was determined to be 30,000

HDFs at day four of culture. Oct4 and Sox2 expression peaked at this size and time and the expression of Nanog was also high. 60,000 HDF spheroids on day five displayed the highest fold change for Nanog. However, this size and time was not considered optimal due to the low levels of Oct4 and Sox2.

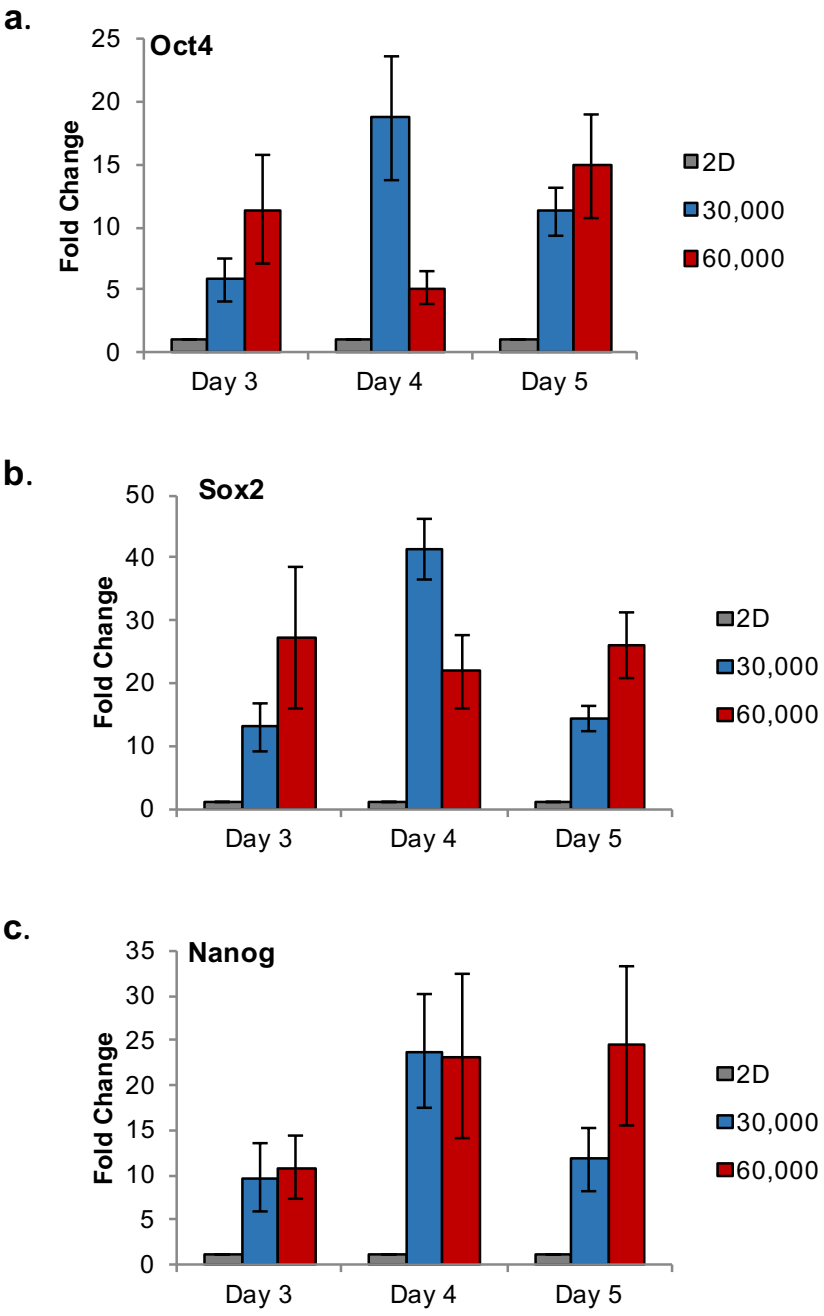

Figure 3.3. QPCR Analysis of Change in Expression of Oct4, Sox2 and Nanog in 3D HDFs Over Time.

HDFs were cultured as 2D monolayers and 3D spheroids with initiating cell numbers of 30,000 and 60,000 cells for up to five days in culture. RNA was extracted from 2D HDFs at 80% confluency on day one and from 120 spheroids on days three-five. cDNA samples were generated and then analysed by QPCR. Expression of Oct4, Sox2 and Nanog for was normalised to expression of the housekeeping gene GAPDH and made relative to expression levels the 2D sample. Fold changes were calculated as 2-ddCt. Data from two HDF cell lines identified in section 2.1.1. were pooled and mean fold changes are shown ± SEM.

3.3 Expression of Mesodermal Markers:

The expression levels of pluripotency factors in MSCs are not as high as in pluripotent stem cells (Pennock et al., 2015) and the 3D MSCs have been identified as mesoderm specific through the expression of mesodermal markers Brachyury, Goosecoid, KDR, CXCR4 and a decrease in CXCL12. Due to these findings the HDFs were also analysed for the expression of markers associated with early germ layer specification. Two separate samples of HDFs from different donors were cultured as monolayers and as 30,000 HDF spheroids for up to five days. RNA was extracted on days three to five. This RNA was then processed as explained in section 2.2 and analysed through QPCR was used to analyse the expression levels of Brachyury, Goosecoid, KDR, CXCR4 and CXCL12 in 3D HDFs compared to 2D HDFs.

Brachyury is a highly conserved gene and transcripts first appear during development at the mid-blastula transition and the highest expression occurs during gastrulation and this is necessary for mesoderm formation (Artinger et al., 1997; Smith et al., 1991). Brachyury is known to have an important role in the development of various tissue types, an example of which is vertebrate development through a Brachyury and canonical Wnt signalling loop and as previously mentioned a lack of Brachyury expression results in a truncated body axis (Martin and Kimelman, 2010). The expression of Brachyury decreases afterwards. This makes Brachyury an early marker for mesoderm formation. The QPCR results for Brachyury showed that by day three there was a 2.5-fold increase in expression when compared to 2D HDFs. By day four there was a further increase of up to 5.5-fold which then continued to decrease on day 5 to approximately a 4.5-fold change (Figure 3.4a). The expression change of most significance is day four as this was the day chosen to be the optimal size and time for dedifferentiation as supported by the data on pluripotency factor expression. Goosecoid is a homeobox-containing gene that is expressed during gastrulation and is thought to be involved in the Spemann's organiser (Artinger et al., 1997; Cho et al., 1991). Expression levels decrease during differentiation which means it can also be used as a marker for mesoderm formation. The QPCR results for Goosecoid showed an increase in expression in 3D compared to 2D HDFs with a 14-fold increase by day three which continued to increase on day four up to 27-fold increase. The expression levels then dropped to a 21-fold increase on day five (Figure 3.4b). This pattern of increase in expression until day four and then a drop in expression on day five follows a similar

pattern that Brachyury expression levels follow but the fold change for Goosecoid is considerably higher (figure 3.4b). Kinase insert domain receptor (KDR) also known as vascular endothelial growth factor receptor 2 (VEGFR2) is found in multipotent mesodermal progenitor cell. These KDR expressing progenitor cells are essential to the formation of the haemangioblast (Shalaby et al., 1995). KDR expression increases in 3D HDFs in comparison to 2D HDFs by approximately 36-fold. The expression levels then continue to increase to 63-fold change on day four and then drops to a 20-fold change on day five. Expression of KDR was considerably higher than both Brachyury and Goosecoid, but follows the same temporal pattern (Figure 3.4c). The mesodermal marker expression data supports day four as the optimal time for HDF dedifferentiation in 3D culture.

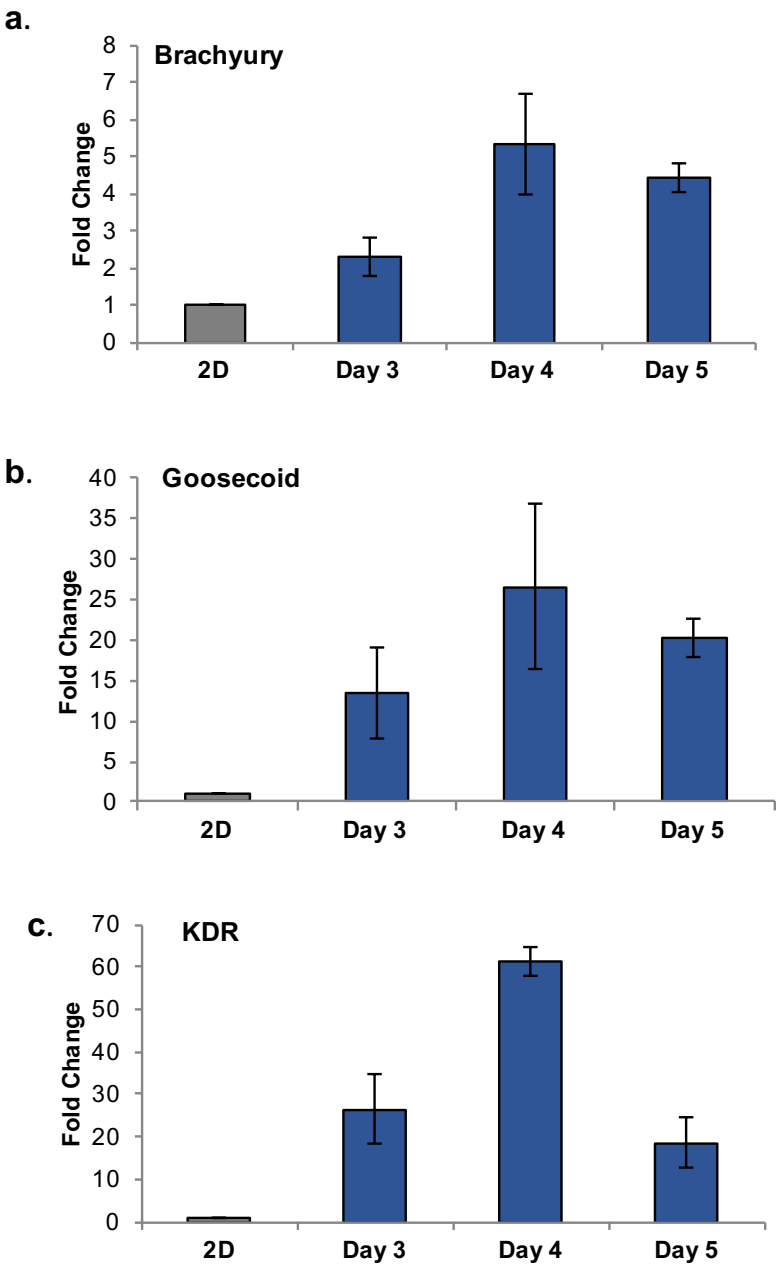

Figure 3.4. QPCR Analysis of Change in Expression of Brachyury, Goosecoid and KDR in 3D HDFs Over Time.

HDFs were cultured as 2D monolayers and 3D spheroids with initiating cell numbers of 30,000 cells for up to five days in culture. RNA was extracted from 2D HDFs at 80% confluency on day one and from 120 spheroids on days three-five. cDNA samples were generated and then analysed by qPCR. Expression of Brachyury, Goosecoid and KDR for was normalised to expression of the housekeeping gene GAPDH and made relative to expression levels the 2D sample. Fold changes were calculated as 2-ddCt. Data from two HDF cell lines identified in section 2.1.1. were pooled and mean fold changes are shown ± SEM.

C-X-C chemokine receptor 4 (CXCR4) is expressed in cells during development and it binds to the corresponding ligand CXCL12 (Sugiyama et al., 2006). It has fundamental roles during organogenesis and is expressed during development in mesoderm and definitive endoderm but not in ectoderm. CXCR4 is involved in dynamic and complementary expression patterns in mesendodermal specification such as the development of neuronal, cardiac, vascular, haematopoetic and craniofacial tissues (McGrath et al., 1999). CXCR4 is also expressed by haematopoietic stem cells and is involved in mediating homing and it is also found in endothelium. Specifically it is often used as a marker of arterial endothelial cell differentiation (Kurian et al., 2013; McGrath et al., 1999; Sugiyama et al., 2006).

CXCR4 decreases during differentiation and specification during development which allows us to use CXCR4 expression as a method of characterising the dedifferentiated state of HDFs that have been cultured in 3D. The pattern of CXCR4 expression does not appear to follow a similar pattern to Brachyury and Goosecoid. CXCR4 expression greatly increases to approximately 1180-fold by day three which is maintained at that level until day five where the expression level drops to around a 210-fold increase (Figure 3.5a). Additionally, the corresponding ligand for CXCR4. CXCL12, which is typically expressed by stromal cells, was found to decrease or be maintained at 2D levels. There was a 0.6-fold decrease in expression by day three which went up to 0.9- and 1.1-fold on days four and five respectively (figure 3.5b). CXCR4 protein was also detected throughout the 3D HDF structure using immunostaining and by western blotting (Figure 3.6 & 3.7). Immunostaining showed a uniform CXCR4 expression on the surface of the cells throughout the section (Figure 3.6). This suggests that the cells spanning from the centre to the outside layers are relatively homogenous. Western blot analysis also showed that CXCR4 expression increased in the 3D HDFs compared to the 2D HDFs (Figure 3.7). Densitometry using Image J and this showed that the intensity of CXCR4 expression by 3D HDF was three times higher than that in 2D HDFs (Figure 3.7b).

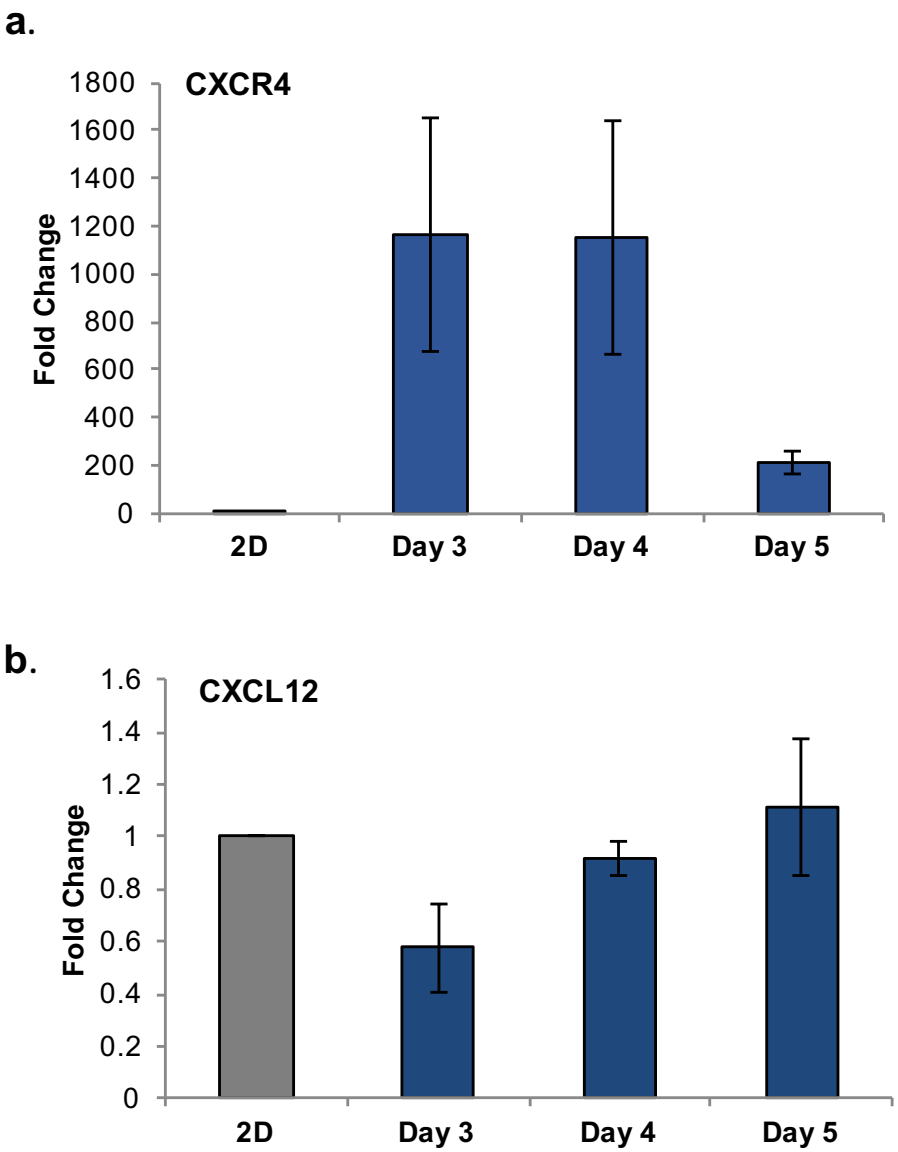

Figure 3.5. QPCR Analysis of Change in Expression of CXCR4 in 3D HDFs Over Time.

HDFs were cultured as 2D monolayers and 3D spheroids with initiating cell numbers of 30,000 cells for up to five days in culture. RNA was extracted from 2D HDFs at 80% confluency on day one and from 120 spheroids on days three-five. cDNA samples were generated and then analysed by QPCR. Expression of CXCR4 for was normalised to expression of the housekeeping gene GAPDH and made relative to expression levels the 2D sample. Fold changes were calculated as 2-ddCt. Data from two HDF cell cultures identified in section 2.1.1. were pooled and mean fold changes are shown ± SEM.

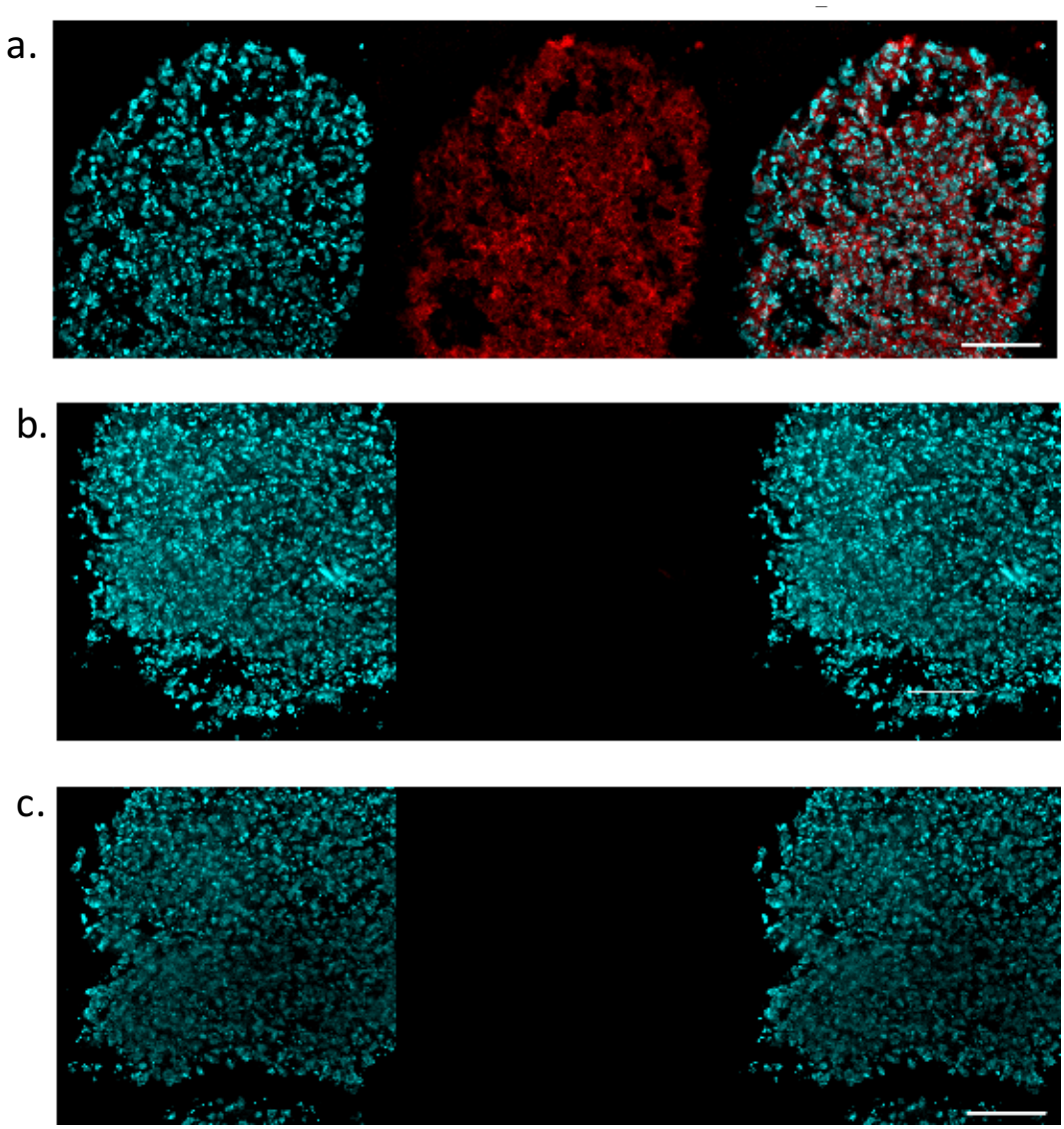

Figure 3.6. Immunostaining of CXCR4 of 3D HDF Sections.

CXCR4 immunostained sections of 3D HDFs (30,000 cells per spheroid, day four) (a). Each sample shows DAPI staining, CXCR4 staining and a merged image. Two controls are shown (b) an isotype control and (c) a secondary antibody control. (Scale bar = 100μm)

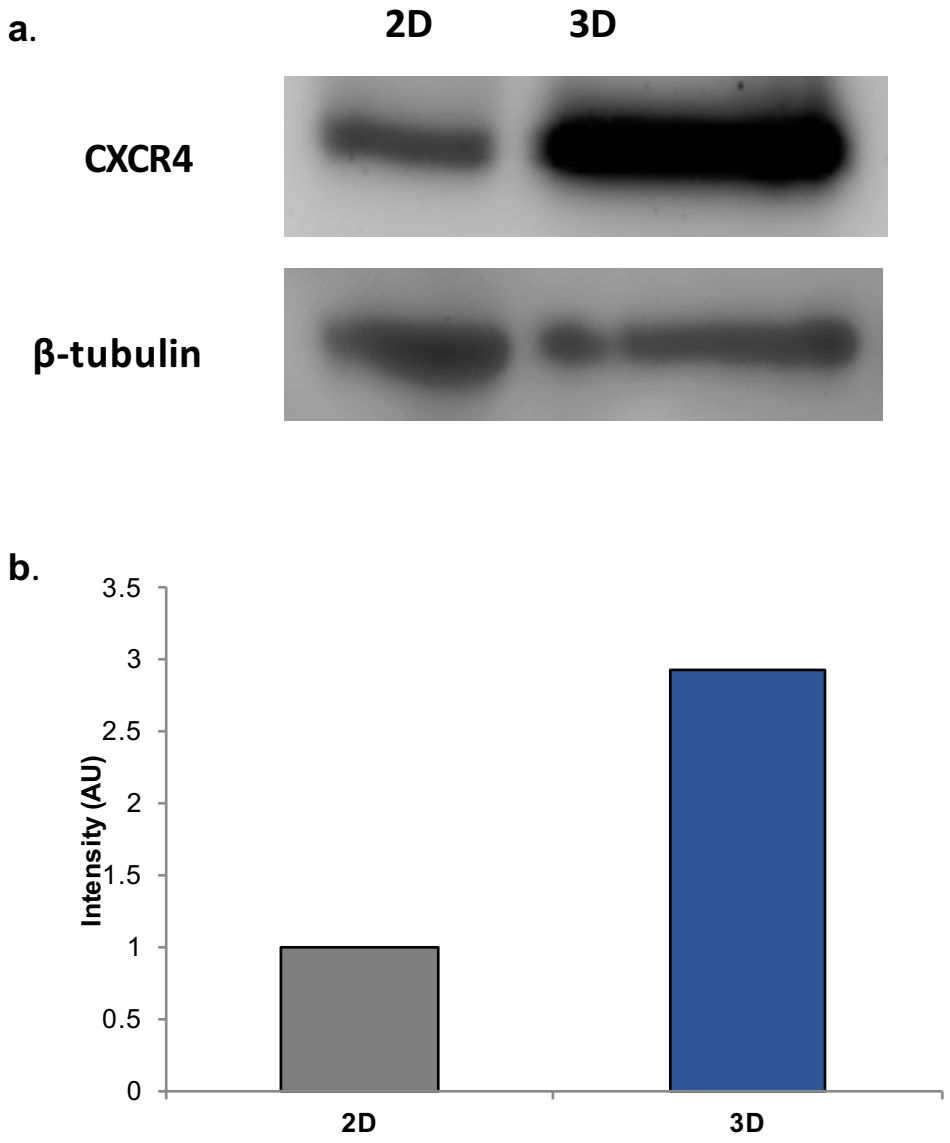

Figure 3.7. Western Blot Analysis of CXCR4 Expression in 2D and 3D HDFs using β-tubulin as a Control.

HDFs were cultured as monolayers and as 30,000 HDF spheroids for four days. Total protein was extracted and analysed by western blot analysis. The membrane was probed using anti-CXCR4 and anti- β-tubulin. The density was measured using ImageJ 3D expression levels were measured relative to 2D and then normalised to β-tubulin. b) Bar chart shows normalised relative intensities. No repeats were done.

3.4 Analysis of Autophagy in 3D HDFs:

It was hypothesised that autophagy could play a role in the 3D HDF dedifferentiation process in a manner similar to 3D MSCs (Pennock et al, 2015) due to the apparent need for cell size shrinkage and cytoplasmic remodelling. An increased autophagic response may also promote cytoplasmic clearance and restructuring required for dedifferentiation to a more primitive state.

The transcription factor EB (TFEB) is a master gene linked to lysosomal biogenesis and plays a major role in expression of autophagy and lysosomal genes (Settembre et al., 2011). HDFs were cultured as monolayers and in 3D culture for up to six days. RNA samples were isolated on days three to five and analysed using QPCR to monitor TFEB expression levels over time as described in section 2.2. It was shown by the third day that a 4-fold change in TFEB upregulation was observed in 3D HDFs compared to 2D HDFs. TFEB expression continued to increase on day four with approximately a 5-fold higher levels than 2D HDFs (Figure 3.8). There was a small decrease in TFEB expression on day five at around 3.5 fold higher than 2D HDFs. These data would suggest that there is an increase in autophagy in the 3D HDFs.

Lysosomal-associated membrane protein 1 (LAMP-1) is a lysosomal glycoprotein found on the surface of lysosomes is thought to be partly responsible in maintaining their integrity (Jw et al., 1985). Lysosomes are a key organelle in the autophagy response as they contain multiple degradative enzymes that are used to digest materials to be cleared from the cell (Eskelinen, 2006). Lysosomes fuse with phagosomes, to aid clearance of unwanted cellular material, by digesting the phagosomal contents. HDFs were cultured as monolayers and as 30,000 HDF spheroids for four days. Protein was extracted and then analysed for LAMP-1 expression by western blotting using beta-tubulin as a loading control (Figure 3.9). 3D HDFs showed LAMP-1 protein expression which when measured using ImageJ showed a 10-fold increase in intensity in the 3D HDFs when compared to the 2D HDFs (figure 3.9b).

3D HDFs were also examined at the ultrastructural level for evidence of cytoplasmic remodelling. HDFs were grown as monolayers and as 30,000 HDF spheroids for four days and then processed and sectioned as described in section 2.1.3. The 3D HDFs were then analysed using transmission electron microscopy (TEM). Multiple

images from the TEM series showed numerous autophagosome- and lysosome-like structures (Figure 3.10). The TEMs also showed mitochondria that were small and rounded which would suggest mitochondrial regression. This may indicate that the 3D HDFs are dedifferentiating and potentially switching from oxidative to glycolytic metabolism as observed in 3D MSCs (Pennock et al,2015).

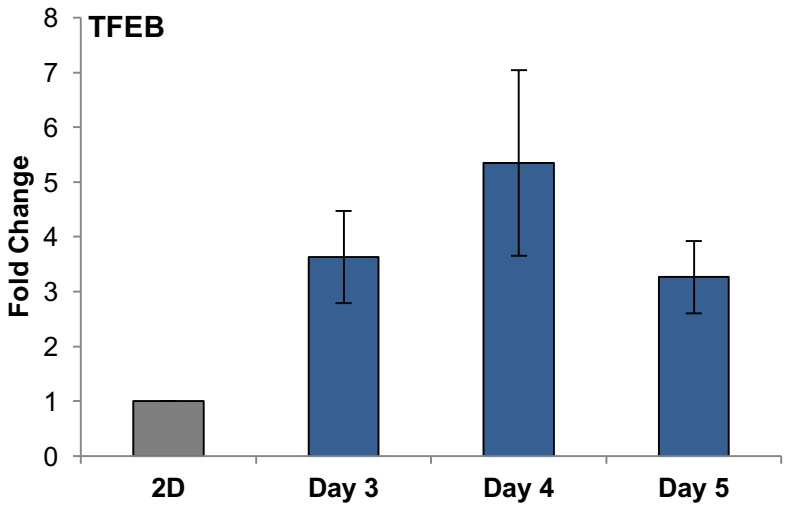

Figure 3.8. QPCR Analysis of Change in Expression of TFEB in 3D HDFs Over Time

HDFs were cultured as 2D monolayers and 3D spheroids with initiating cell numbers of 30,000 cells for up to five days in culture. RNA was extracted from 2D HDFs at 80% confluency on day one and from 120 spheroids on days three-five. cDNA samples were generated and then analysed by QPCR. Expression of TFEB for was normalised to expression of the housekeeping gene GAPDH and made relative to expression levels the 2D sample. Fold changes were calculated as 2-ddCt. Data from two HDF cell cultures identified in section 2.1.1. were pooled and mean fold changes are shown ± SEM.

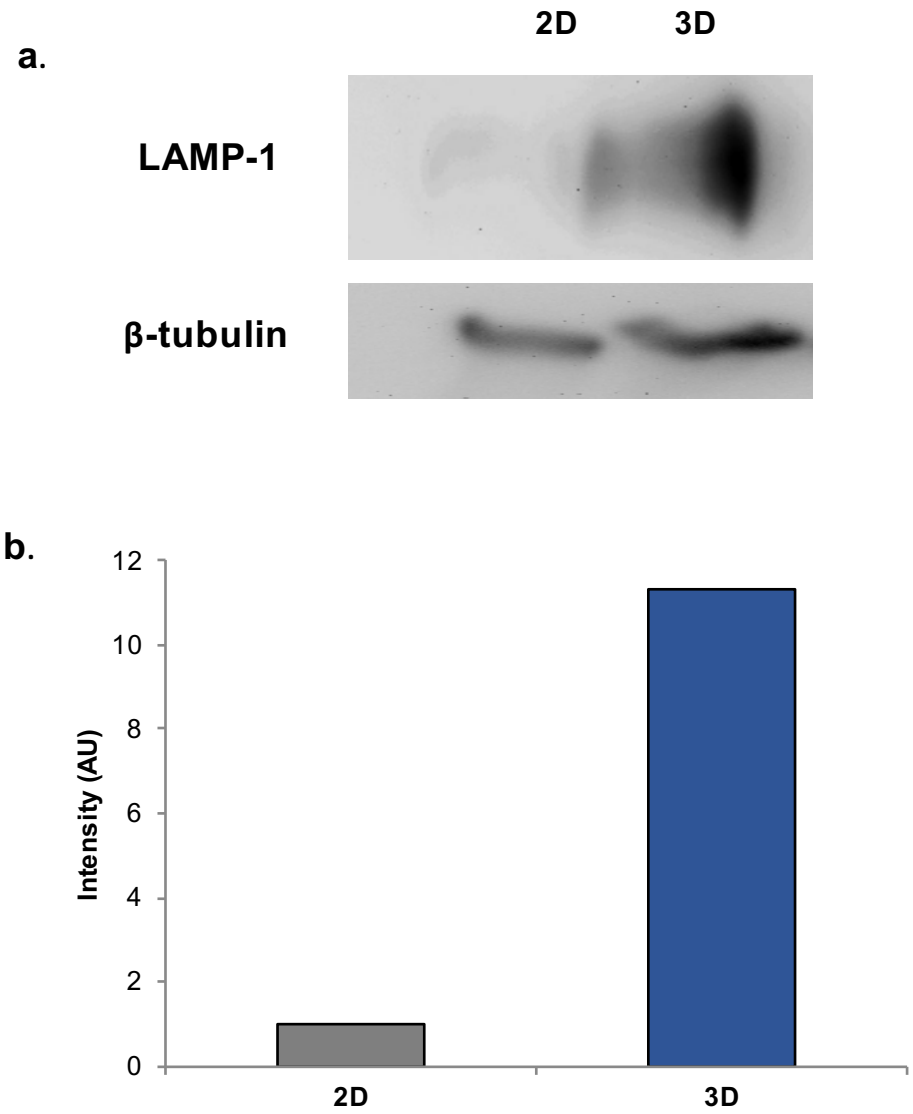

Figure 3.9. Western Blot Analysis of LAMP-1 Expression in 2D and 3D HDFs using β-tubulin as a Control.

HDFs were cultured as monolayers and as 30,000 HDF spheroids for four days. Total protein was extracted and analysed using western blot. The membrane was probed using anti-LAMP-1 and anti- β-tubulin antibodies. The density was measured using Image J software, 3D levels were measured relative to 2D and then normalised to β-tubulin. b) Bar chart shows normalised relative intensities. No repeats were done.

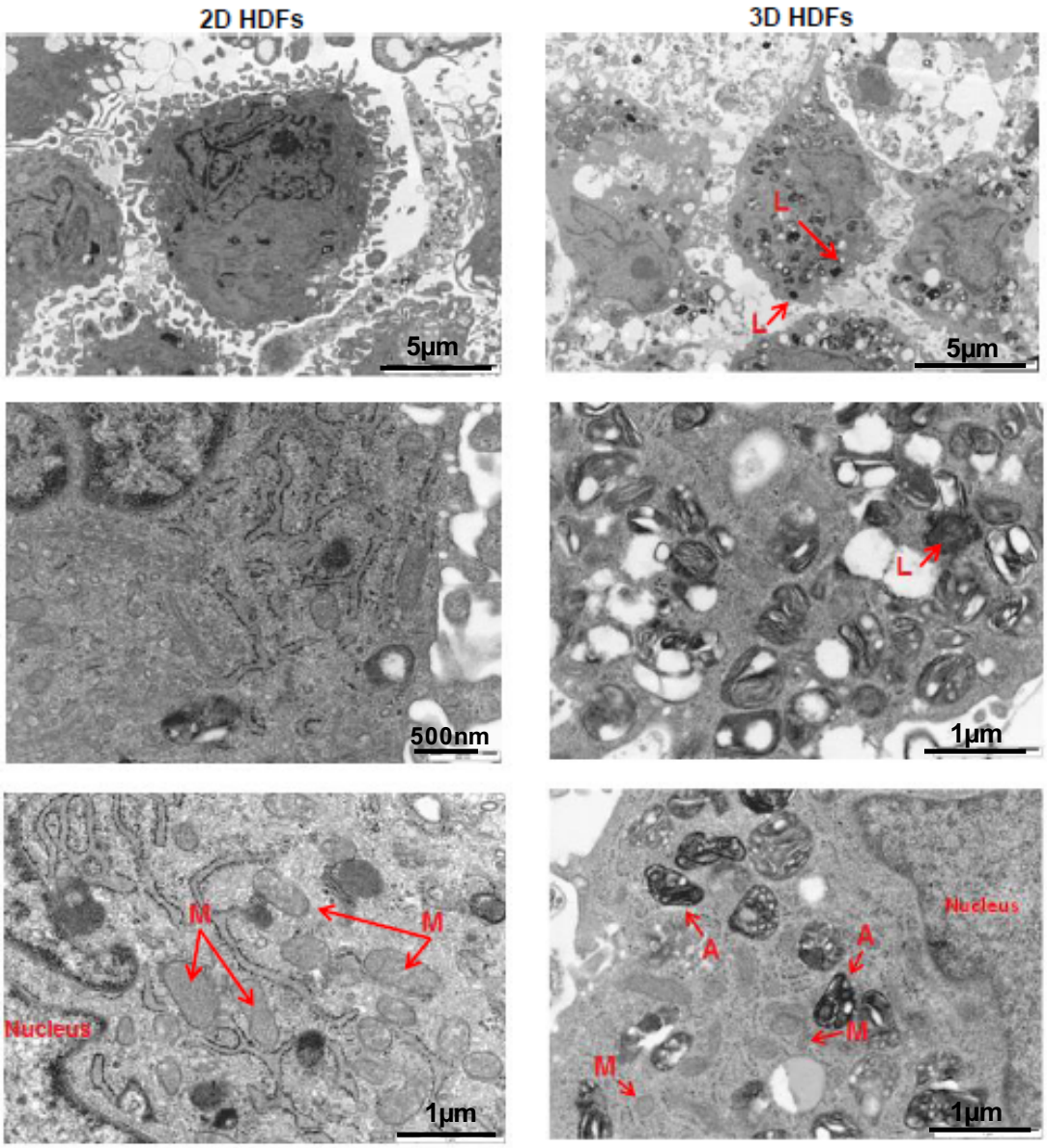

Figure 3.10. Transmission Electron Microscopy Images of 2D and 3D HDFs.

HDFs were cultured as a 2D monolayer and as 3D HDF spheroids. The spheroids were then sectioned and stained and examined by transmission electron microscopy (TEM). TEM images show smaller rounded mitochondria (M) and numerous lysosome (L) and autophagosomes-like (A) structures.

3.5 Redifferentiation of the 3D HDFs Into an Endothelial-like Cells:

3.5.1 3D HDF Network-like Formation:

The potential of dedifferentiated cells to become new cell types is essential to develop the use of these cells for regenerative purposes. The fact that the 3D HDFs appear to be dedifferentiating to what is thought to be a mesoderm-like state suggests that these cells should be able to differentiate into cell types originating from this lineage. The potential of the 3D HDFs to switch to different mesendodermal cell types was tested by growing them in endothelial cell differentiation conditions. HDFs were grown as monolayers and as 30,000 3D HDF spheroids for four days. The 3D HDFs were then disaggregated and cultured in EGM on Matrigel to determine their ability to form endothelial-like cells. A typical characteristic of endothelial cells grown on Matrigel is the formation of vascular network-like structures (Voyta et al., 1984) This is seen by the multiple different types of endothelial cell such as HUVECs. The introduction of Matrigel creates an extracellular matrix which mimics aspects of a 3D cellular environment which induces the formation of capillary-like structures (Kleinman and Martin, 2005). Initially the cells were grown in EGM1 (Promocell) which is a specific medium that does not contain FBS but specific endothelial cell growth supplements including FGF-2. The disaggregated 3D HDFs are plated at approximately 500,000 cells/ml on 200µl Matrigel (see section 2.7). Images of the network-like structures were taken using a LCM filter setting on a Leica DC 500 microscope (Figure 3.11). Additionally, after seven days of 3D HDFs being cultured on Matrigel, the actin cytoskeleton was stained using rhodamine-phalloidin to help visualise the capillary-like structures and to determine the penetrative distance of the 3D HDFs (Figure 3.12) Four z-stacks were taken from four different wells and the average distance was measured was around 322µm. The 3D HDFs took approximately seven days to form networks whereas the 2D HDFs initially spread across the well and then retracted to form aggregations on the Matrigel (Figure 3.11b). The formation of these capillary-like structures by 3D HDFs suggests they are capable of differentiating into an endothelial-like cell. The networks formed by the 3D HDFs and HUVECs are different as HUVECs are known to form capillary-like structures on the surface of the Matrigel. However, the 3D HDFs appear to have increase penetrative potential and form networks through approximately 300µm of Matrigel. The cells formed fine connections that appeared to predominantly consist of cell-cell

connections whereas HUVECs appeared to aggregate together to form longer capillary-like structures.

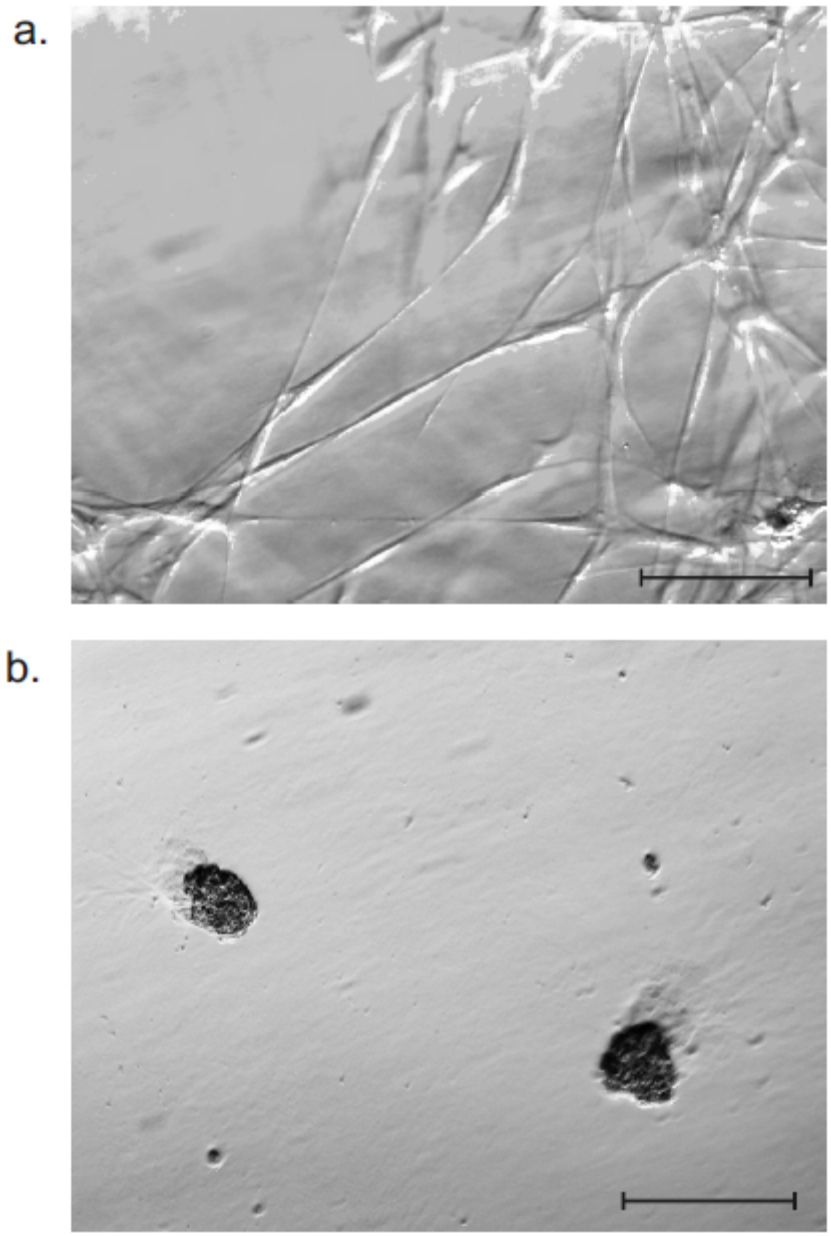

Figure 3.11. LCM images of 3D HDFs Grown on Matrigel in Endothelial Cell Media 1.

LCM images of 3D HDFs cultured in Matrigel for seven days (a). LCM images of 2D HDFs cultured on Matrigel for seven days (b). Images were taken using LCM filter on a Leica DC 500 scale bar is 50μm. Experiment was replicated 6 times and repeated once and the pictures are representative of each experiment.

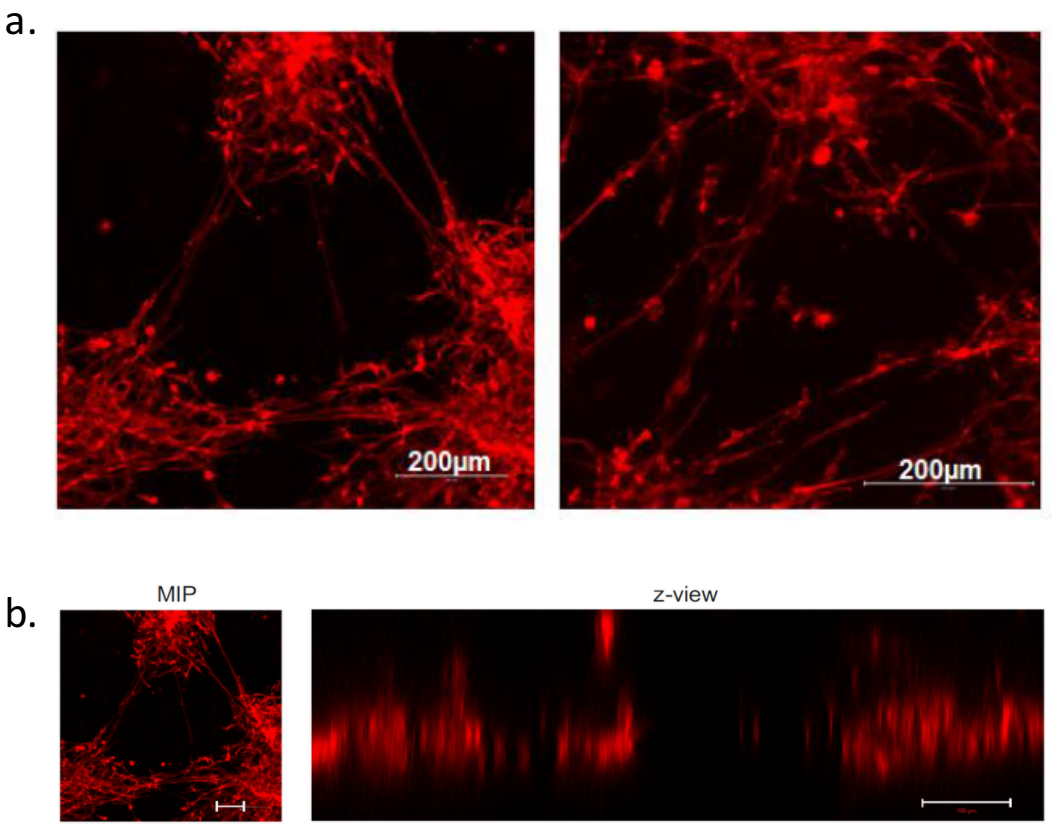

Figure 3.12. Maximum Projection Intensity Images of Rhodamine-Phalloidin Stained 3D HDFs Grown on Matrigel in Endothelial Cell Media 1.

3D HDFs cultured in Matrigel for seven days and cells were stained with rhodamine-phalloidin. Rhodamine-phalloidin images were taken as a z-stack due to the formation of a multi-layered 3D network and the images were combined to create a maximum intensity projection, scale bar is 200µm (a). Using the rhodamine-phalloidin z-stack images the penetration distance of the cells could be measured, scale bar is 100 µm (b). Experiment was replicated 3 times in separated wells and images are representative of each replicate. However, the experiment was not repeated.

Vascular endothelial growth factor (VEGF) and in particular VEGF-A, is a key regulator of vasculogenesis, VEGF-A signals through fms-related tyrosine kinase-1 (Flt-1) or kinase insert domain receptor (KDR). It also interacts with co-receptors neuropilin-1 and -2 (Nrp-1, Nrp-2) (Marcelo et al., 2013). VEGF has been shown to be a key regulator in endothelial cell differentiation as shown in *in vitro* differentiation experiments (Nourse et al., 2010). Many reports suggest that 50ng/ml of VEGF is the optimal concentration for endothelial cell differentiation and production of functional endothelium and it has also been shown that a combination of VEGF and FGF-2 is essential for endothelial cell differentiation, as explained in the Introduction, section 1.6. (Chen et al., 2009; Wang et al., 2010, 2013). This would suggest that the addition of VEGF to the protocol could potentially promote the induction of endothelial cell differentiation from 3D HDFs.

This was also hypothesised of Bone Morphogenetic Protein 4 (BMP4) which is a key signalling component that is important for mesoderm specification but also mesoderm differentiation toward endothelial and haematopoietic cell fates. BMP4 along with FGF-2 is known to play a role in cell commitment towards a KDR+ progenitor cell which then had the capacity to differentiate down a venous/arterial development path or the lymphogenesis pathway. BMP4 knock out mice embryos showed that mesoderm formation does not occur without BMP4 (Winnier et al., 1995). It has been shown that short-term BMP4 treatment initiated mesoderm induction at high efficiency in hES cells (Zhang et al., 2008). This would suggest that combination of BMP4 and VEGF could promote differentiation towards a mixed population of endothelial-like cells. BMP4 is present to initiate mesoderm formation focussing towards endothelial/haematopoietic progenitor cell and VEGF is known to promote endothelial differentiation.

The network forming experiment was repeated using EGM2 (Promocell) which contained 20ng/ml IGF1, 0.5ng/ml VEGF and 10x the original concentration of FGF-2 (10ng/ml). Additionally, this media was supplemented with increased VEGF (50ng/ml) and BMP4 (10ng/ml) separately and combined to test whether these supplements would improve the formation of the network-like structures. The disaggregated 3D HDFs were grown in EGM2 and the supplemented forms EGM 3-5 the method and concentrations of supplements added can be found in section 2.7. Brightfield images were taken at 5x magnification and 20x magnification of the network structure at 24 hours (Figure 3.13). The additional supplements appeared to have decreased the time required for the 3D HDFs to form networks. There was also a visual difference in the networks formed when the 3D HDFs were grown with

additional supplements. The 3D HDFs now formed networks that appeared more like aggregates of cells forming larger longer networks. The addition of a combination of VEGF and BMP4 also showed sprouting along the networks which is indicative of endothelium (Figure 3.13). The behaviour of these 3D HDFs is similar to that of HUVECs grown in a same condition. The 2D HDFs grown in the same conditions formed huge cell aggregates and no networks with and without the additional supplements images were taken using the Leica LCM setting as it provided the clearest images due the 3D nature of the aggregations (Figure 3.14).

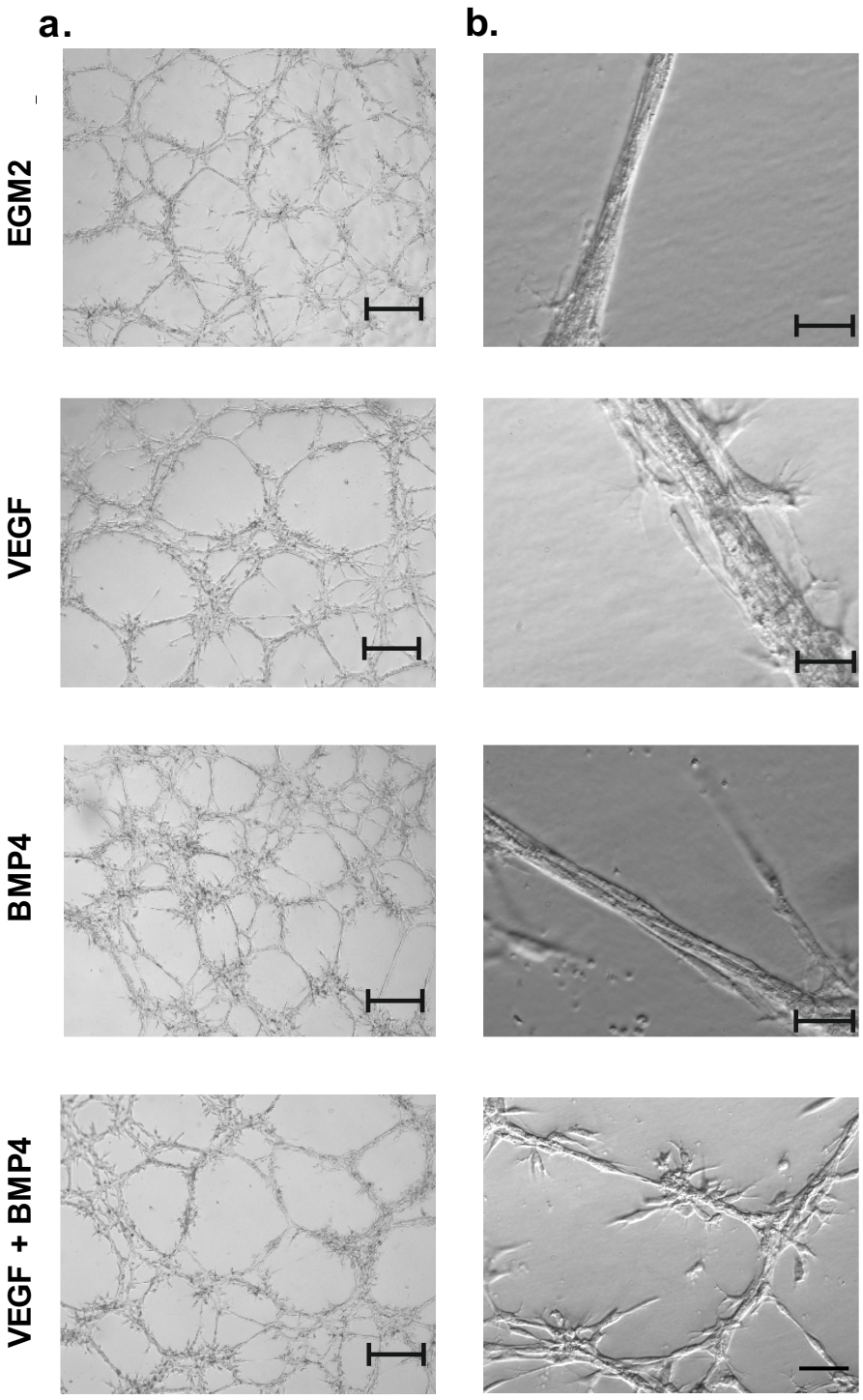

Figure 3.13. Brightfield Images of 3D HDF Network-Formation

Brightfield images of 3D HDFs cultured in Matrigel for 24 hours in different endothelial growth media scale bar = 250μm (a) scale bar = 50μm (b). Images were taken using a Leica DC 500 microscope. Experiment was repeated three times and the pictures are representative of the three repeats.

.

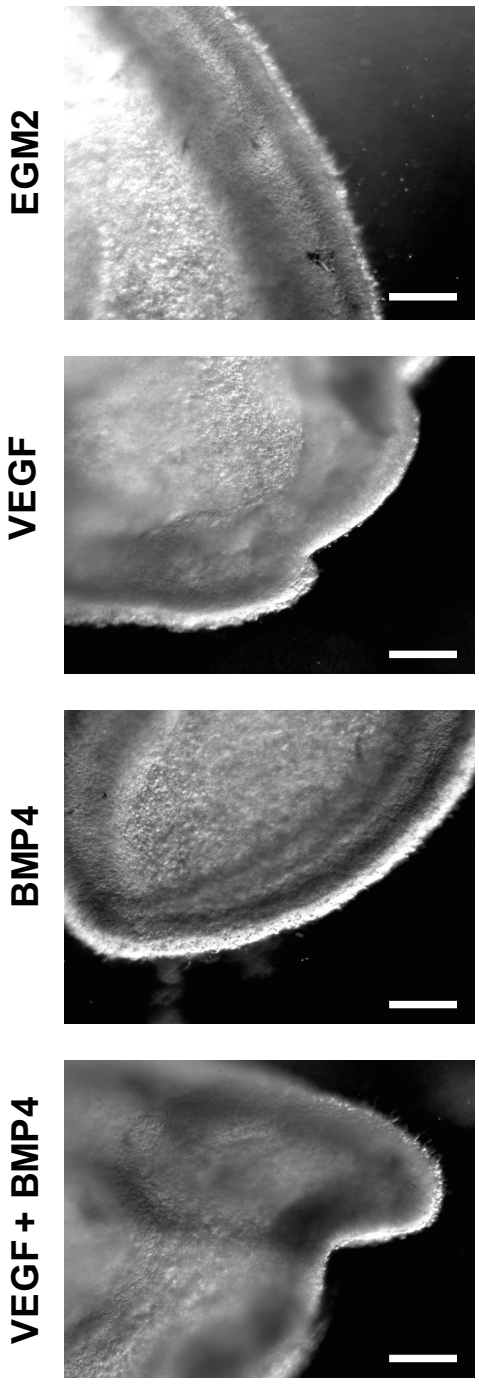

Figure 3.14. Leica LCM Images of 2D HDFs Grown on Matrigel

LCM images of 500,000 2D HDFs cultured on Matrigel for 24 hours in different endothelial growth media. Images were taken using the LCM filter on a Leica DC 500, scale bar = 250μm. Experiment was repeated twice and the pictures are representative of those repeats.

3.5.2 Comparison of Network Structures of 3D HDFs:

The brightfield images of the 3D HDFs grown in endothelial growth conditions were used in order to measure the lengths and the widths of the capillary-like structures in order to compare the networks formed (Figure 3.15). The addition of high concentrations of VEGF all showed statistically significant differences when the EGM media is altered. EGM2 produced shortest capillary-like structures and the addition of high concentrations of VEGF appeared to produce the longest capillary-like structures. It would also appear that the addition of BMP4 has an effect on the length of the capillaries as they appear to increase with the additional BMP4.

The width of the capillary-like structures were also measured using the brightfield images. The capillaries made by the cells grown in EGM2 were the shortest but were measured to be the second thickest. Whereas the addition of high concentrations of VEGF that showed the longest capillaries were also the thinnest. It would also appear that the addition of BMP4 increases the width of the capillary-like structures. It could be speculated the addition of certain concentrations of VEGF and BMP4 may encourage differentiation into different endothelial cell subtypes.

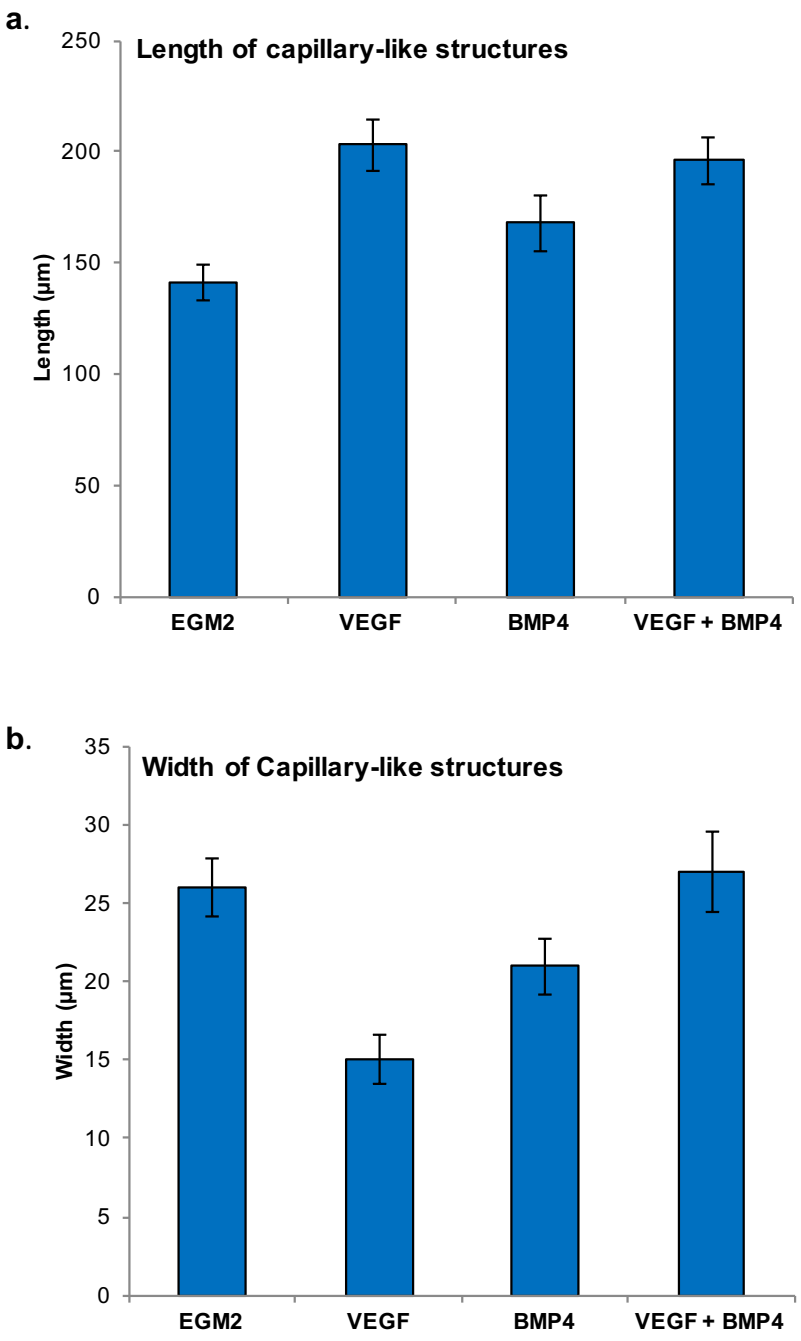

Figure 3.15. Quantification of 3D HDF Capillary-like Structures.

HDFs were cultured as 3D spheroids with initiating cell numbers of 30,000 cells for up to four days in culture. The cells were then disaggregated as described in section 2.6. and grown on Matrigel in EGM2 and supplemented EGM2 for 24 hours. The capillary-like structures were measured using Image J to compare their length (a) and width (b) n=35 and mean lengths and widths are shown ± SEM.

3.5.3 AcLDL Uptake of the 3D HDFs:

Finally, another test that was done to determine whether the 3D HDFs have functional characteristics similar to the HUVECs was to measure the acLDL uptake of the 3D HDFs. The 3D HDFs and HUVECs were grown on Matrigel as described in section 2.9 until the networks form and acLDL was then added and incubated for five hours. The results show that the 3D HDFs are not up taking acLDL to the same level of the HUVECs (Figure 3.16). This would suggest that despite the fact a small amount of acLDL uptake can be seen the cells do not have all the characteristics of endothelial cells and suggests alterations to the differentiation protocol could lead to the 3D HDFs having more endothelial-like characteristics and higher expression levels of the endothelial cell markers.

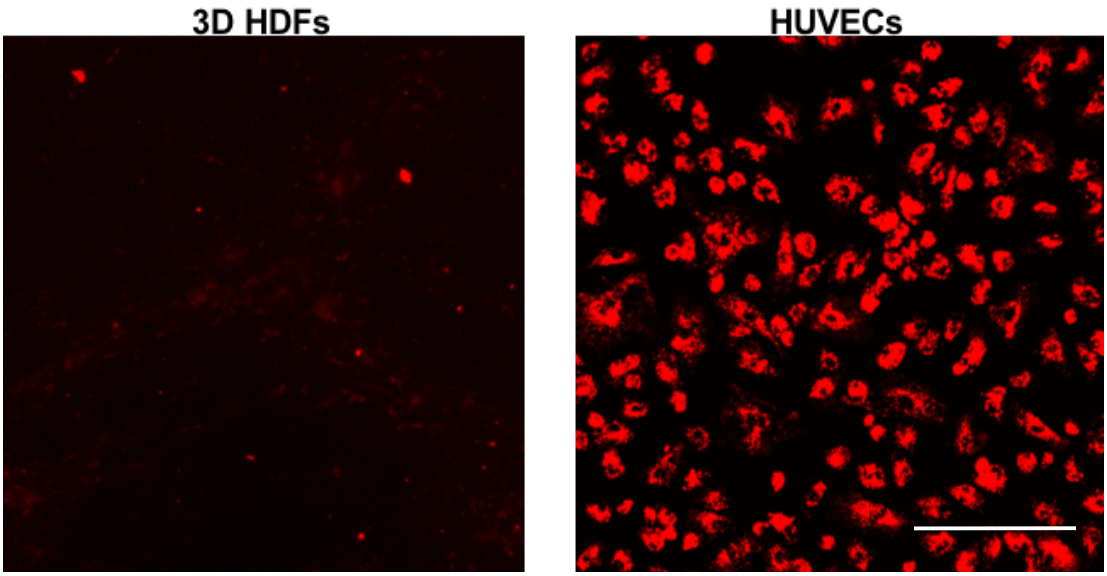

Figure 3.16 acLDL Uptake of 3D HDFs Grown in EGM1.

3D HDFs cultured in Matrigel for seven days and HUVECS cultured in Matrigel for 1 day and both were incubated with 50µl Dil-acLDL for five hours. The images were taken as a z-stack due to the formation of a multi-layered 3D network and the images were combined to create a maximum intensity projection (scale bar is 200µm).

3.5.4 3D HDF Expression of Endothelial Markers:

Due to the fact the 3D HDFs were able to form extensive networks on Matrigel, the cells were tested for their expression of markers typically expressed by endothelial cells. 2D and 3D HDFs grown on Matrigel in EGM1, EGM2 and EGM2 with additional supplements (section 2.7) were cultured and RNA was taken at 48 hours and prepared as described in section 2.2. Using QPCR the expression levels of early endothelial markers such as Kinase Insert Domain (KDR), Neuropilin-1 (Nrp-1), Neuropilin-2 (Nrp-2), Activin receptor-like kinase (ALK1), Ephrin-type B receptor 4 (EphB4) and vascular endothelial Cadherin (VE-Cadherin) were analysed.

Cadherins are one of the major cell adhesion molecule families and they are defined by the typical extracellular cadherin domains (EC-domain) that are capable of binding through a homophillic calcium-dependent interaction. There are two types of cadherins type I such as E- N- P- and C-cadherin and type II which lack the HAV motif which is a binding motif found in the EC domain of type I cadherins. It is to this group that VE-cadherins belong (Vestweber, 2008). VE-Cadherin is known to interact with KDR which is important for cell signalling events. This is most likely critical for counter regulation of VEGF-stimulated proliferation and regulation of apoptosis (Carmeliet et al., 1999; Lampugnani et al., 2003). The KDR-VE-cadherin complex is also important during the regulation of VE-cadherin mediated adhesion during VEGF-stimulated angiogenic processes (Lambeng et al., 2005). Increases in tyrosine phosphorylation of KDR and VE-cadherin by VEGF has been proven to be involved in endothelial cell migration as well as tubular formation (Lin et al., 2003). The expression of VE-Cadherin was either maintained at 2D levels or upregulated slightly. The EGM containing both BMP4 and the increased VEGF concentration had the highest VE-Cadherin expression which was seen to be around 1.5-fold (Figure 3.17a). This is only a moderate increase and other factors had much higher fold changes. However, EGM containing only high concentrations of VEGF showed a decrease in VE-Cadherin expression. This suggests the BMP4 is essential for the endothelial differentiation protocol.

Activin receptor-like kinase (ALK1) is a type I receptor for transforming growth factor β (TGFβ) and is important in determining vascular development during angiogenesis. ALK1 was found to be expressed in blood vessels and through knock-out experiments it has been shown that a lack of ALK1 is fatal during embryonic development due to hyperdilation and hyperfusion of blood vessels (Corti et al., 2011; Urness et al., 2000). Interestingly ALK1 has been shown to have a

paradoxical effect as it has been shown to have an involvement in cell proliferation and tubule formation (Valdimarsdottir et al., 2002). However, when a constitutively active form is expressed in endothelial cells, it is found to prevent proliferation and have an effect in angiogenic maturation (Lamouille et al., 2002). This suggests that ALK1 has opposing roles that are dosage dependent during development. As ALK1 expression is restricted to endothelial cells, receptor upregulation of ALK1 it can be used as a marker of endothelial differentiation. The expression levels of ALK1 appeared to increase the most in the media containing only the additional BMP4 where an 8-fold increase was seen (Figure 3.17b). The other forms of the media appear to show a maintenance of ALK1 expression or have very minor increases when compared to the 2D HDFs.

Neurophilin-2 (Nrp-2) is also found to form a complex with VEGFR2 (KDR) and VEGFR3. It is thought to lower the activation threshold of these receptors to increase sensitivity to specific VEGF isoforms (Favier et al., 2006). Nrp-2 expression has been reported to be restricted to vein and lymphatic vessel vascular membranes. It has been shown to have a prominent role in VEGF mediated angiogenesis. Nrp-2 is expressed in early endothelial cells and can be used to determine whether the cells are differentiating to an endothelial-like cell. Nrp-2 has a moderate increase in expression by 1.5-fold in 3D HDFs grown in unsupplemented media and the media containing both VEGF and BMP4 (Figure 3.17c). However, the addition of VEGF and BMP4 separately appeared to increased the levels of Nrp-2 the most by approximately 3-fold.

Neuropilin-1 (Nrp-1) is known to be expressed in very early differentiation of stem cells that have begun the process of forming vascular, haematopoetic and cardiac precursors. Nrp-1 is known to be involved in endothelial cell differentiation through its capacity to form complexes with VEGFR1 and KDR (VEGFR2) (Gelfand et al., 2014). KDR as previously mentioned is a marker of endothelial cell differentiation through its very important role as a VEGF receptor. Nrp-1 expression is known to to be a marker for endothelial precursors that form functional vessels and its expression coincides with Brachyury expression (Cimato et al., 2009). KDR and Nrp-1 bind to create a complex and enhances the ability of KDR to bind specific VEGF isoforms and VEGF-mediate chemotaxis (Gelfand et al., 2014). Nrp-1 has been concluded to be an early marker of endothelial cells and can also be used to look at the differentiation of the 3D HDFs. Unsupplemented medium showed very little change in Nrp-1 expression. The 3D HDFs in the two media with BMP4 increased the most with a 3-fold increase in expression (Figure 3.17d).

Eph receptors and their ligands comprise the largest family of receptor tyrosine kinases. Eph receptors and their ligands are involved in mediating multiple developmental processes. They are known to be involved in neuronal guidance, cardiac development, tissue-border formation and are expressed by endothelial cells (Gerety et al., 1999; Hamada et al., 2003; Wang and Anderson, 1997). EphB receptors have been shown to have crucial roles in vascular morphogenesis as evidenced using knock-out experiments (Hamada et al., 2003). These experiments have shown that EphB is essential since arterio-venous differentiation is disturbed when EphB receptors are not present. Ephrin-B2 is a marker of arterial endothelial cells and EphB4 is expressed by venous endothelial cells (Hamada et al., 2003). This was shown by experiments involving signalling between EphB4 and Ephrin-B2 ligand which have shown they are involved in mediating signalling between arterial and venous endothelial cells to allow proper morphogenesis and differential growth of arterial and venous vessels (Hamada et al., 2003; Wang et al., 1998). This allows us to use EphB4 as a marker of endothelial cell differentiation and more specifically venous endothelial cell differentiation. The 3D HDFs grown in the VEGF and BMP4 supplemented EGM showed a 73-fold increase in EphB4 expression in comparison to the 2D HDFs (Figure 3.17e). It would appear that the addition of both BMP4 and VEGF is essential to the high EphB4 expression as the other growth conditions showed very little EphB4 change.

KDR was previously used to identify whether the 3D HDFs were dedifferentiating to a mesoderm specific cell. KDR is also typically found on endothelial progenitor cells and on fully differentiated endothelial cells. Maintenance of KDR expression in the 3D HDFs grown in endothelial cell growth conditions would provide supporting evidence that the cells are not regaining their typical HDF characteristics and an upregulation would indicate that the 3D HDFs are differentiating to an endothelial-like cell. However, by this time KDR expression had decreased below the levels of 2D HDFs and was shown to decrease to about 0.5-fold (Figure 3.17f). However, through the addition of 50ng/ml VEGF, 10ng/ml BMP4 and 20ng/ml of IGF1 it was possible to increase the levels of KDR to 115-fold (Figure 3.17f). This fold-change is higher than the KDR expression increase in just 3D HDFs before being grown in endothelial growth conditions which suggests they are beginning to differentiate and that the additional supplements are necessary for endothelial differentiation.

The addition of both VEGF and BMP4 appears to have been the most successful endothelial differentiation media. The 3D HDFs were capable of forming network-like structures on Matrigel in this media. The networks were measured to be the longest

and thickest which could suggest they are the most stable. The 3D HDFs grown in EGM2 with additional VEGF and BMP4 also had the highest VE-Cadherin, EphB4 and KDR fold-changes. The other endothelial markers also all appeared to increase with the exception of ALK1. This suggests these endothelial growth conditions were the most successful.

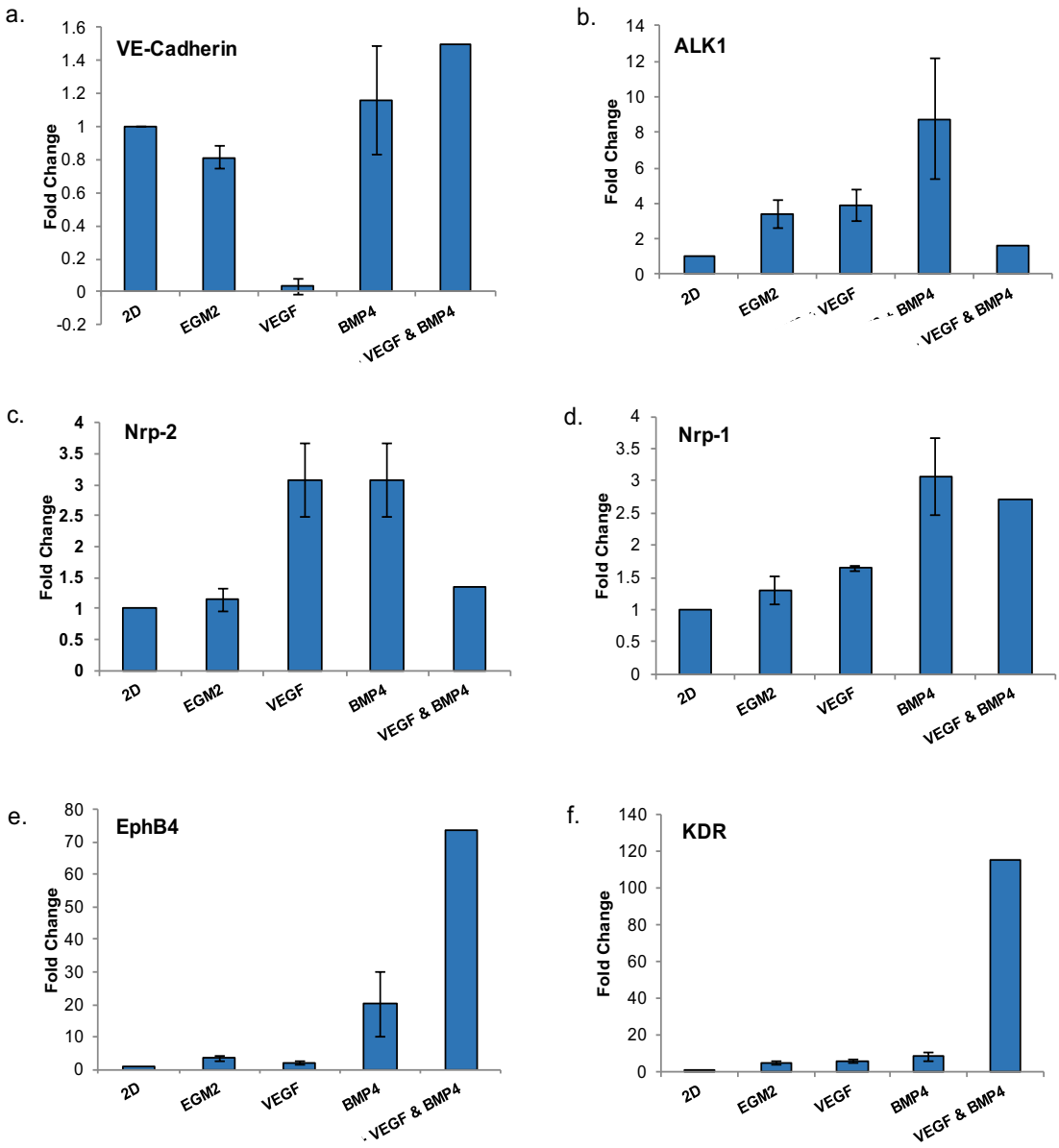

Figure 3.17. QPCR Analysis of Change in Expression of Endothelial Markers in 3D HDFs Grown in Endothelial Growth Conditions

HDFs were cultured as 2D monolayers and 3D spheroids with initiating cell numbers of 30,000 cells for up to five days in culture. The cells were then disaggregated as described in section 2.6. and grown on Matrigel in EGM, EGM with VEGF, EGM with BMP4 and EGM with both VEGF and BMP4. RNA samples were taken at 48 hours and cDNA samples were generated and expression of endothelial cell markers VE-Cadherin (a), ALK1 (b), Nrp-2 (c), Nrp-1 (d), EphB4 (e) and KDR (f) were analysed by QPCR. Endothelial markers were normalised to expression of the housekeeping gene GAPDH and made relative to expression levels the 2D sample. Fold changes were calculated as 2-ddCt. Data from two series of experiments were pooled and mean fold changes are shown ± SEM (with the exception of the VEGF & BMP4 media).

4 Discussion

4.1 Characterisation of 3D HDFs:

The experimental evidence provided suggests that HDFs cultured in specific 3D conditions dedifferentiated to an early mesodermal cell. Additionally, evidence was also provided showing that these cells are then able to redifferentiate to endothelial-like cells. The TEMs of the 3D HDFs showed smaller rounded mitochondria which is different to the 2D HDFs which have an elongated tubular morphology similar to what was seen in the 3D MSCs (Pennock et al., 2015). This could be evidence that the HDFs are undergoing a similar metabolic switch. However, there was not enough time to perform additional experiments to confirm the hypothesis of this metabolic switch by itself. The observation of smaller rounded mitochondria is not enough evidence to clearly establish a metabolic switch but leads to speculation that it occurs in the 3D HDFs which could be confirmed by further experiments. The 3D HDFs also express upregulated expression levels of Brachyury, Goosecoid, KDR and CXCR4 when compared to 2D HDFs. Thus, we can conclude that the cells are responding to the culture technique in a similar manner to that of the 3D MSCs and are potentially dedifferentiating to a similar stage of cellular development. It is proposed that the 3D HDFs could have similar properties to this early germ layer specification to the haemangioblast stage. This idea is supported further by observation that Goosecoid expression is only expressed briefly during development as opposed to Brachyury which is downregulated much later (Artinger et al., 1997; Blum et al., 1992). In 3D HDFs Brachyury is upregulated approximately 5.5-fold in the 3D culture conditions. Brachyury is a key regulator for mesoderm formation and is expressed in all nascent mesoderm and then downregulated when cells begin to specify. It is therefore, essential to characterization of these cells, and suggests an early stage of mesodermal development. Additionally, Goosecoid was also upregulated in the 3D HDFs by approximately 26.5-fold and is also expressed in mesendoderm. In comparison to the expression of Brachyury, Goosecoid is only expressed for a short period of time during development, which would suggest that the 3D HDFs are broadly equivalent to an early mesendodermal cell type. Another reason which suggests that these cells are at the pre-haemangioblastic stage is the finding that they express upregulated levels of KDR by approximately 61-fold. KDR is typically expressed in cells destined to become haemangioblastic cells which will then carry on to form haematopoietic stem cells and endothelial cells. In the haemangioblastic stage and the stages leading up to it, both KDR and Brachyury

are known to be expressed (Fehling, 2003). However, despite the high level of expression of Brachyury in early mesoderm formation, it is downregulated at the start of the haemangioblastic stage in order to aid in cell specification. This downregulation of Brachyury is controlled by KDR expression. Further evidence of 3D HDF dedifferentiation is supported further by the findings concerning upregulation of CXCR4 which is typically expressed during development of haematopoietic stem cells and specific endothelial cells and has been shown to be a marker of the haemangioblast (McLeod et al., 2006). CXCR4 mRNA and protein expression was upregulated in 3D HDFs versus 2D HDFs and was shown to be expressed throughout the spheroid by immunostaining. In addition mRNA expression of the CXCR4 ligand and stromal marker CXCL12 decreased in the 3D HDFs. Further analysis of the mesodermal markers could be done in order to quantify the number of cells that are dedifferentiating. Collectively, however, these analyses of marker expression do support the dedifferentiation from a fully differentiated adult cell to an early mesoderm-like status.

4.2 Autophagy Levels in the 3D HDFs

Previous work with MSCs has suggested that autophagy could play a principal role in 3D-induced dedifferentiation *in vitro* (Pennock et al., 2015). It was proposed that specific 3D culture conditions helped to control autophagy at a sub-lethal level that favoured rejuvenation and promoted cellular reorganisation and clearance of the cytoplasmic components. The link between dedifferentiation and autophagy is becoming better understood. It has been shown *in vitro* that cells that undergo induction of pluripotency also have increased levels of autophagy (Menendez et al., 2011). The mechanism is thought to involve the removal of mitochondria that have aged and are potentially producing damaging reactive oxidative species. This accelerates the ability of the cells to switch to glycolytic metabolism which is a requirement for reprogramming (Menendez et al., 2011). The results presented here also provide evidence for an increase in autophagy in HDFs grown using the 3D culture technique. This was indicated by the increased mRNA expression of TFEB an autophagy master gene, and the increased expression of the lysosomal LAMP-1 protein; both these observations were also made previously in the 3D MSCs (Pennock et al., 2015). Other proteins were analysed in the 3D MSCs such as the LC3:LC2 ratio. This could be done in the future in the 3D HDFs as it gives more evidence that the 3D HDFs also have an increased level of autophagy.

TEMs were also taken of 2D and 3D HDFs which provided visual evidence of intracellular alterations. The primary differences between the two culture methods can be seen by the increased numbers of autophagosome- and lysosome-like structures throughout the 3D HDFs, which were absent in 2D HDFs. However, due to the fact the TEMs were only visually interpreted, the structures could be fully identified by staining for typical autophagy-related organelles such as lysosomes. There also appeared to be more debris surrounding the 3D HDFs when compared to the 2D HDFs, the nature of which is yet to be determined. The results regarding the increase in autophagy for 3D HDFs are at a preliminary stage. Therefore, more experiments would be needed to confirm that autophagy levels are increasing in the 3D HDFs. However, due to the fact the 3D MSCs have been shown to have increased levels of autophagy through a variety of techniques (Pennock et al., 2015), we can hypothesise that 3D HDFs also undergo a similar dedifferentiation process through controlled autophagy.

Furthermore, the combination of the results showing spheroid condensation, which is evidence of reversal to an early mesoderm-like cell type corresponding with an upregulation of autophagy. This strongly suggests that the 3D HDFs and the 3D MSCs follow the same or closely related dedifferentiation process.

4.3 Comparisons with Natural Regeneration:

The blastema is a key component in regeneration in multiple organisms and the process appears to be very similar between species. Planarians are a type of flatworm that is capable of regenerating. Planarians have the three germ layers and are acoelomate (solid body with no body cavity) (Reddien et al., 2005). Planaria can be dissected and then the separate pieces can regenerate into a complete organism (Reddien and Sánchez Alvarado, 2004). This is also done through the formation of a blastema similar to the process of regeneration used by newts and salamanders (Reddien and Sánchez Alvarado, 2004; Reddien et al., 2005). The method in which blastemal regeneration occurs is still not fully understood. However, specific aspects have been elucidated due to studies in multiple lower organisms and similarly to the blastema formation in zebrafish, it has also been shown that autophagy plays a role in planarian regeneration (Reddien and Sánchez Alvarado, 2004). Broad comparisons can be made between the 3D *in vitro* culture model used here and the formation of the blastema during limb regeneration. Blastemal cells are thought to be mainly mesenchymal cells and potentially other cell types that have

dedifferentiated to a multipotent stem cell. Therefore, the cells are not classed as pluripotent and cannot form a whole new embryo. This is also because the cells retain memory of their type as they enter the blastema structure and therefore can only become cell types from that specific lineage (King and Newmark, 2012). This probably accounts for regeneration of the limb without the formation of unwanted tissues, which is a property of pluripotent stem cells. Interestingly, both the 3D MSCs and 3D HDFs have increased but low level mRNA expression of pluripotency factors which differs to blastemal cells which have not been shown to express Oct4 or Nanog. However, blastemal cells been shown to have upregulated Sox2 expression (Monaghan et al., 2012). Another broad similarity between the 3D HDFs and blastemal cells is upregulated mesodermal markers including Brachyury, KDR and CXCR4. This increased mesodermal marker expression corresponds with analyses of blastemal cells in axolotls, which has shown that certain processes are upregulated including mesodermal development (Monaghan et al., 2012).

An interesting aspect that has not been studied extensively is the role of autophagy in blastemal cells during regeneration in multiple organisms including planarian regeneration and zebrafish caudal fin regeneration. It has been shown using autophagy-defective zebrafish that there was more apoptotic cell death and the surviving cells then failed to express the markers typically expressed during differentiation to form the fin (Varga et al., 2014). They were also incapable of re-growing the surgically removed fin which provides supporting evidence that autophagy is a key process in injury-induced regeneration in lower organisms (Varga et al., 2014). Evidence has also been provided showing that increased numbers of autophagosomes are seen during Hydra tip regeneration (Galliot, 2006) and treating Hydra with autophagy inhibitors delays regeneration. It is thought that the stress of amputation causes the increase in autophagy. However, due to the fact that a large amount of autophagy causes rapid cell death, it is necessary for Hydra to limit the amount of autophagy. Although there are fewer similarities between Hydra Regeneration and the 3D system there are still a few parallels. Both 3D MSCs and 3D HDFs have shown evidence of increased levels of autophagy which suggests they could be undergoing a similar process and it is also thought to be controlled through time and size in culture. Additionally, the 3D MSCs were grown in 3D with bafilomycin which prevents autophagy from occurring and it was seen that the spheroids do not form properly suggesting that autophagy is a key regulator of 3D culture based dedifferentiation (Pennock et al., 2015) which is similar to the need for autophagy for blastema dedifferentiation.

Clearly there remain differences between blastemal cells and 3D HDFs as the processes are not identical and the methods used to generate 3D HDFs was not an attempt to mimic blastemal formation. Similarities include spheroid condensation, increased Sox2 expression, mesodermal marker upregulation and the necessity for increased autophagy are nevertheless observed. Therefore, the process in which blastemal cells are dedifferentiating could provide further clues about the nature of the process that is occurring in the spheroid structure.

4.4 Endothelial-like Cell Differentiation:

The ability for the dedifferentiated 3D HDFs to re-differentiate into different cell types is necessary to test the dedifferentiated status of the 3D HDFs and to explore the potential for new cell therapies. As the 3D HDFs display early mesodermal features, the differentiation protocol chosen was for endothelial cell differentiation. The endothelium is a single cell layer that lines blood vessels and a key factor for inflammatory responses, vasomotor tone and vascular permeability. It also plays a pathogenic role in cardiovascular diseases such as atherosclerosis and its consequences, such as heart attacks and strokes. Stem cell biology potentially opens up new opportunities to understand endothelial development and function and offers the opportunity to produce more of this tissue for use in therapy. This could also include preventative measures to strengthen or rejuvenate the existing endothelium. This has previously been referred to as therapeutic angiogenesis is a new approach to treating cardiovascular disease and cardiomyopathy (Reed et al., 2013).

iPSC differentiation to both early endothelial cells and mature endothelial cells such as the cells found in the endothelium has been achieved by many laboratories (Choi et al., 2009; Homma et al., 2010; Kurian et al., 2013; Li et al., 2011). It has been shown that endothelial differentiation using iPSCS requires an initial differentiation to a mesodermal progenitor or endothelial progenitor cell and can then be differentiated further into endothelial progenitor cells or mature endothelial cells. However, this process can take up to two weeks to develop endothelial progenitor cells (Asahara et al., 1997; Choi et al., 2009; Hristov et al., 2003; Marcelo et al., 2013). Additionally, having to produce a progenitor cell usually requires the need to sort for cells expressing cell surface markers in order to generate a more homogenous final population of endothelial cells (Kurian et al., 2013), which can be

a lengthy and inefficient process. The 3D HDFs were used in an endothelial cell differentiation protocol in an attempt to create an early mixed population of endothelial-like cells. The need for an initial mesodermal progenitor differentiation stage, followed by cell sorting was avoided due to the fact that the cells were not dedifferentiated to a pluripotent state.

The ability for endothelial cells to form networks on Matrigel is well known and used to characterize cells that have been differentiated alongside other characteristics to identify whether the cells are phenotypically similar to actual endothelial cells (Belair et al., 2015). This is essential as endothelial cells differentiated *in vitro* need to be able to reproduce functional properties in order to be characterized as an actual endothelial cell. It has been shown previously that using VEGF/KDR signalling iPSC derived endothelial cells can produce networks on Matrigel (Belair et al., 2015) and that other artificial endothelial cells such as the HDFs that were transdifferentiated are also capable of forming these networks on Matrigel (Sayed et al., 2014). The VEGF/KDR signalling molecules have been shown to key in angiogenesis and the formation of networks have been shown to be dependent on VEGF *in vivo* (Belair et al., 2015). The data using the 3D HDFs showed very limited capacity to form networks in the media without VEGF which would be expected as there is no VEGF/KDR signalling to induce angiogenesis. The networks formed without the addition of VEGF were small and the 3D HDFs appeared to form protrusions to create cell-cell adhesions. This is different to the networks formed by mature endothelial cells such as HUVECs where the individual networks consist of multiple aggregated HUVECs to create larger and longer capillary-like structures (Saunders and Hammer, 2010). In comparison 3D HDFs that were cultured in the presence of VEGF were capable of forming by 24 hours. This suggests the networks forming were being created due to the VEGF/KDR signalling, especially as the cells in the presence of high concentrations of VEGF appeared to have higher KDR expression. Lower and higher concentrations of VEGF were used and the differences between the networks can be analysed. These results showed that dependent on what supplements were added to the media the capillary-like structures were different lengths and widths. The addition of VEGF appears to form longer thinner capillaries whereas BMP4 seems to form shorter slightly thicker capillaries. The media containing the combination of VEGF and BMP4 formed comparatively medium length and the thickest capillary-like structures. There has not been any explanation as to why these factors are having these effects on the structure of the networks and it could be hinting that the different supplements are favouring different subtypes of

endothelial cells. The findings presented here are extremely encouraging, however evidence of network-forming capacity does not alone demonstrate an endothelial phenotype. For example, some cancer cell have been shown to be capable of forming networks on Matrigel such as brain tumour U87 cells, melanoma B16F1 cells and breast cancer MDA-MB-435 cells in a cell number dependent manner. This is due to the fact that some cancer cells have vasculogenic activity that is independent of endothelial-cell associated angiogenesis (Francescone III et al., 2011). Therefore, other methods are necessary to determine whether these cells are re-differentiating to an endothelial-like cell. Acetylated-low density (acLDL) uptake is used as a method to characterize endothelial cells. The 3D HDFs that were grown in unsupplemented media were tested for their ability to uptake acLDL. The HUVECs showed very high acLDL uptake, whereas the 3D HDFs did not appear to have increased uptake of acLDL. If additional time had been available, the 3D HDFs grown in EGM with VEGF and BMP4 would also be tested for increased acLDL uptake. Therefore, increased acLDL uptake was not confirmed in the 3D HDFs grown in the improved endothelial differentiation protocol. Finally, the expression of endothelial markers is also essential to confirming the 3D HDFs are re-differentiating to endothelial-like cells. The 3D HDFs are shown to have increased expression of VE-Cadherin, Nrp-1, Nrp-2, ALK1, EphB4 and KDR which are factors known to be expressed by endothelial cells and are also used in other differentiation studies (Kurian et al., 2013; Sayed et al., 2014). The differentiation protocol appears to needs further optimisation such as additional time in culture and additional supplements or concentration alterations in order to potentially increase the endothelial marker expression. However, the evidence suggests the cells could be on the path to becoming an early mixed population of endothelial progenitor cells.

5 Future work and Conclusions:

Further experimentation will be required before finally and conclusively elucidating the processes that occur in the 3D HDFs. To analyse metabolic shift, the cells could be tested for loss of mitochondrial activity or the media could be tested for glucose uptake and lactate production. Additionally, more functional evidence of autophagy could be sought to confirm fully that the 3D HDFs are also undergoing the same autophagy-mediated dedifferentiation process as the 3D MSCs. However, the focus of the present research was the overall process of lineage-conversion from HDFs to endothelial cells. Finally, as previously mentioned the endothelial differentiation

protocol requires some adjustments to improve the results. The key factors that need altering are optimising the differentiation protocol time and altering angiogenic supplement concentration, particularly BMP4 and FGF-2, and potentially including other factors to improve the extent of endothelial differentiation, such as TGF-beta

The results presented here suggest that adult HDFs are capable of undergoing 3D-based dedifferentiation to an early mesodermal progenitor cell-like developmental stage (Figure 5.1). The 3D HDFs appear to have increased levels of autophagy, which may assist cytoplasmic restructuring and intracellular renovation. Finally, there is evidence that the dedifferentiated 3D HDFs are capable of undergoing re-differentiation into endothelial-like cells, as shown by the expression of a range of endothelial cell markers and most impressively, the formation of capillary-like networks on Matrigel (Figure 5.1). Once this protocol has been refined further this protocol could potentially contribute to developing new cell therapies.

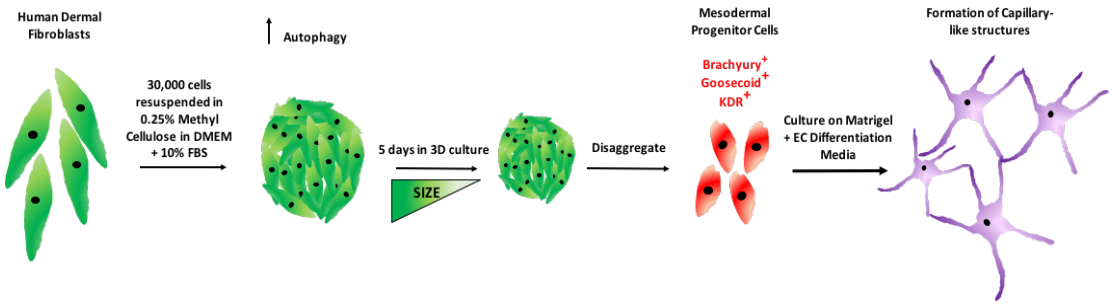

Figure 5.1. Dedifferentiation of Human Dermal Fibroblasts in 3D Culture.

HDFs undergo dedifferentiation to an early mesendoderm-like state when grown as 3D spheroid cultures in a size- and time-dependent manner. HDFs are grown in 96-well U-bottomed plates in 0.25% methyl cellulose in DMEM for four days at 37°C and 5% CO_2. The mesodermal progenitor cells are then capable of undergoing differentiation to an endothelial-like cell that is capable of forming capillary-like structures on Matrigel.

6 Abbreviations:

1. **KDR/VEGFR2:** Kinase insert domain/ Vascular Endothelial Growth Factor Receptor 2
2. **Nrp-1:** Neuropilin-1
3. **Nrp-2:** Neuropilin-2
4. **ALK1:** Activin receptor-like Kinase
5. **EphB4:** Ephrin-type B receptor 4
6. **VE-Cadherin:** Vascular Endothelial Cadherin
7. **FGF-2:** basic fibroblast growth Factor
8. **EGF:** endothelial growth factor
9. **IGF1:** insulin-like growth factor 1
10. **BMP4:** bone morphogenetic protein 4
11. **VEGF:** Vascular endothelial growth factor
12. **LAMP-1:** Lysosomal-associated membrane protein 1
13. **TFEB:** Transcription Factor EB
14. **CXCR4:** chemokine receptor 4
15. **CXCL12:** chemokine ligand 12 (Stromal cell-derived factor 1)
16. **CD31:** cluster of differentiation 31 (Platelet endothelial cell adhesion molecule)
17. **p38 MAPK:** p38 mitogen-activated protein kinases
18. **TLR3**: Toll-like receptor 3
19. **MLV:** murine leukemia virus
20. **HIV:** Human Immunodeficiency virus
21. **BSA:** Bovine Serum Albumin
22. **DMEM:** Dulbecco Modified Eagles Medium
23. **FBS:** Foetal Bovine Serum
24. **P/S:** penicillin and streptomycin
25. **RPMI:** Roswell Park Memorial Institute medium
26. **PBS:** Phosphate Buffer Saline
27. **EGM:** Endothelial Growth Media
28. **ICM:** Inner Cell Mass
29. **HDF:** Human Dermal Fibroblast
30. **MSC:** mesenchymal stromal cell
31. **iPSC:** induced pluripotent stem cell
32. **mESC:** mouse embyronic stem cell
33. **HUVEC:** human umbilical vein endothelial cell
34. **TEM:** Transmission Electron Microscopy
35. **qPCR:** quantitative polymerase chain reaction
36. **AcLDL**: Acetylated-low density lipoprotein

7 References:

1. Adler, H.S., Kubsch, S., Graulich, E., Ludwig, S., Knop, J., and Steinbrink, K. (2007). Activation of MAP kinase p38 is critical for the cell-cycle-controlled suppressor function of regulatory T cells. Blood *109*, 4351–4359.

2. Ambrosino, C., and Nebreda, A.R. (2001). Cell cycle regulation by p38 MAP kinases. Biol. Cell *93*, 47–51.

3. Artinger, M., Blitz, I., Inoue, K., Tran, U., and Cho, K.W.Y. (1997). Interaction of goosecoid and brachyury in Xenopus mesoderm patterning. Mech. Dev. *65*, 187–196.

4. Asahara, T., Murohara, T., Sullivan, A., Silver, M., Zee, R. van der, Li, T., Witzenbichler, B., Schatteman, G., and Isner, J.M. (1997). Isolation of Putative Progenitor Endothelial Cells for Angiogenesis. Science *275*, 964–966.

5. Avilion, A.A., Nicolis, S.K., Pevny, L.H., Perez, L., Vivian, N., and Lovell-Badge, R. (2003a). Multipotent cell lineages in early mouse development depend on SOX2 function. Genes Dev. *17*, 126–140.

6. Avilion, A.A., Nicolis, S.K., Pevny, L.H., Perez, L., Vivian, N., and Lovell-Badge, R. (2003b). Multipotent cell lineages in early mouse development depend on SOX2 function. Genes Dev. *17*, 126–140.

7. Belair, D.G., Whisler, J.A., Valdez, J., Velazquez, J., Molenda, J.A., Vickerman, V., Lewis, R., Daigh, C., Hansen, T.D., Mann, D.A., et al. (2015). Human vascular tissue models formed from human induced pluripotent stem cell derived endothelial cells. Stem Cell Rev. *11*, 511–525.

8. Ben-David, U., and Benvenisty, N. (2011). The tumorigenicity of human embryonic and induced pluripotent stem cells. Nat. Rev. Cancer *11*, 268–277.

9. Bibel, M., Richter, J., Schrenk, K., Tucker, K.L., Staiger, V., Korte, M., Goetz, M., and Barde, Y.-A. (2004). Differentiation of mouse embryonic stem cells into a defined neuronal lineage. Nat. Neurosci. *7*, 1003–1009.

10. Blum, M., Gaunt, S.J., Cho, K.W.Y., Steinbeisser, H., Blumberg, B., Bittner, D., and De Robertis, E.M. (1992). Gastrulation in the mouse: The role of the homeobox gene goosecoid. Cell *69*, 1097–1106.

11. Boroviak, T., Loos, R., Bertone, P., Smith, A., and Nichols, J. (2014). The ability of inner-cell-mass cells to self-renew as embryonic stem cells is acquired following epiblast specification. Nat. Cell Biol. *16*, 513–525.

12. Botha, J.F., Langnas, A.N., Campos, B.D., Grant, W.J., Freise, C.E., Ascher, N.L., Mercer, D.F., and Roberts, J.P. (2010). Left lobe adult-to-adult living donor liver transplantation: Small grafts and hemiportocaval shunts in the prevention of small-for-size syndrome. Liver Transpl. *16*, 649–657.

13. Breier, G., Albrecht, U., Sterrer, S., and Risau, W. (1992). Expression of vascular endothelial growth factor during embryonic angiogenesis and endothelial cell differentiation. Development *114*, 521–532.

14. Brockes, J.P. (1997). Amphibian Limb Regeneration: Rebuilding a Complex Structure. Science *276*, 81–87.

15. Brockes, J.P., and Kumar, A. (2002). Plasticity and reprogramming of differentiated cells in amphibian regeneration. Nat. Rev. Mol. Cell Biol. *3*, 566–574.

16. Carmeliet, P., Lampugnani, M.-G., Moons, L., Breviario, F., Compernolle, V., Bono, F., Balconi, G., Spagnuolo, R., Oosthuyse, B., Dewerchin, M., et al. (1999). Targeted Deficiency or Cytosolic Truncation of the VE-cadherin Gene in Mice Impairs VEGF-Mediated Endothelial Survival and Angiogenesis. Cell *98*, 147–157.

17. Chang, C., and Hemmati-Brivanlou, A. (1998). Cell fate determination in embryonic ectoderm. J. Neurobiol. *36*, 128–151.

18. Chen, W., and Frangogiannis, N.G. (2010). The role of inflammatory and fibrogenic pathways in heart failure associated with aging. Heart Fail. Rev. *15*, 415–422.

19. Chen, M.-Y., Lie, P.-C., Li, Z.-L., and Wei, X. (2009). Endothelial differentiation of Wharton's jelly–derived mesenchymal stem cells in comparison with bone marrow–derived mesenchymal stem cells. Exp. Hematol. *37*, 629–640.

20. Cho, K.W., Blumberg, B., Steinbeisser, H., and De Robertis, E.M. (1991). Molecular nature of Spemann's organizer: the role of the Xenopus homeobox gene goosecoid. Cell *67*, 1111–1120.

21. Choi, K., Kennedy, M., Kazarov, A., Papadimitriou, J.C., and Keller, G. (1998). A common precursor for hematopoietic and endothelial cells. Dev. Camb. Engl. *125*, 725–732.

22. Choi, K.-D., Yu, J., Smuga-Otto, K., Salvagiotto, G., Rehrauer, W., Vodyanik, M., Thomson, J., and Slukvin, I. (2009). Hematopoietic and Endothelial Differentiation of Human Induced Pluripotent Stem Cells. STEM CELLS *27*, 559–567.

23. Cimato, T., Beers, J., Ding, S., Ma, M., McCoy, J.P., Boehm, M., and Nabel, E.G. (2009). Neuropilin-1 identifies endothelial precursors in human and murine embryonic stem cells before CD34 expression. Circulation *119*, 2170–2178.

24. Conrad, C.H., Brooks, W.W., Hayes, J.A., Sen, S., Robinson, K.G., and Bing, O.H.L. (1995). Myocardial Fibrosis and Stiffness With Hypertrophy and Heart Failure in the Spontaneously Hypertensive Rat. Circulation *91*, 161–170.

25. Correia, K.M., and Conlon, R.A. (2000). Surface ectoderm is necessary for the morphogenesis of somites. Mech. Dev. *91*, 19–30.

26. Corti, P., Young, S., Chen, C.-Y., Patrick, M.J., Rochon, E.R., Pekkan, K., and Roman, B.L. (2011). Interaction between alk1 and blood flow in the development of arteriovenous malformations. Development *138*, 1573–1582.

27. Danese, S., Dejana, E., and Fiocchi, C. (2007). Immune regulation by microvascular endothelial cells: directing innate and adaptive immunity, coagulation, and inflammation. J. Immunol. Baltim. Md 1950 *178*, 6017–6022.

28. David T Corr, C.L.G.-B. (2009). Biomechanical behavior of scar tissue and uninjured skin in a porcine model. Wound Repair Regen. Off. Publ. Wound Heal. Soc. Eur. Tissue Repair Soc. *17*, 250–259.

29. De Val, S., and Black, B.L. (2009). Transcriptional Control of Endothelial Cell Development. Dev. Cell *16*, 180–195.

30. Dimanlig, P.V., Faber, S.C., Auerbach, W., Makarenkova, H.P., and Lang, R.A. (2001). The upstream ectoderm enhancer in Pax6 has an important role in lens induction. Development *128*, 4415–4424.

31. Engel, F.B., Schebesta, M., Duong, M.T., Lu, G., Ren, S., Madwed, J.B., Jiang, H., Wang, Y., and Keating, M.T. (2005). p38 MAP kinase inhibition enables proliferation of adult mammalian cardiomyocytes. Genes Dev. *19*, 1175–1187.

32. Eskelinen, E.-L. (2006). Roles of LAMP-1 and LAMP-2 in lysosome biogenesis and autophagy. Mol. Aspects Med. *27*, 495–502.

33. Fausto, N. (2000). Liver regeneration. J. Hepatol. *32, Supplement 1*, 19–31.

34. Fausto, N., and Campbell, J.S. (2003). The role of hepatocytes and oval cells in liver regeneration and repopulation. Mech. Dev. *120*, 117–130.

35. Favier, B., Alam, A., Barron, P., Bonnin, J., Laboudie, P., Fons, P., Mandron, M., Herault, J.-P., Neufeld, G., Savi, P., et al. (2006). Neuropilin-2 interacts with VEGFR-2 and VEGFR-3 and promotes human endothelial cell survival and migration. Blood *108*, 1243–1250.

36. Fehling, H.J. (2003). Tracking mesoderm induction and its specification to the hemangioblast during embryonic stem cell differentiation. Development *130*, 4217–4227.

37. Folmes, C.D.L., Nelson, T.J., Martinez-Fernandez, A., Arrell, D.K., Lindor, J.Z., Dzeja, P.P., Ikeda, Y., Perez-Terzic, C., and Terzic, A. (2011). Somatic Oxidative Bioenergetics Transitions into Pluripotency-Dependent Glycolysis to Facilitate Nuclear Reprogramming. Cell Metab. *14*, 264–271.

38. Francescone III, R.A., Faibish, M., and Shao, R. (2011). A Matrigel-Based Tube Formation Assay to Assess the Vasculogenic Activity of Tumor Cells. J. Vis. Exp. JoVE.

39. Frenz, D.A., Jaikaria, N.S., and Newman, S.A. (1989). The mechanism of precartilage mesenchymal condensation: A major role for interaction of the cell surface with the amino-terminal heparin-binding domain of fibronectin. Dev. Biol. *136*, 97–103.

40. Galliot, B. (2006). Autophagy and Self-Preservation: A Step Ahead from Cell Plasticity? Autophagy *2*, 231–233.

41. Gelfand, M.V., Hagan, N., Tata, A., Oh, W.-J., Lacoste, B., Kang, K.-T., Kopycinska, J., Bischoff, J., Wang, J.-H., and Gu, C. (2014). Neuropilin-1 functions as a VEGFR2 co-receptor to guide developmental angiogenesis independent of ligand binding. eLife *3*, e03720.

42. Gerety, S.S., Wang, H.U., Chen, Z.-F., and Anderson, D.J. (1999). Symmetrical Mutant Phenotypes of the Receptor EphB4 and Its Specific Transmembrane Ligand ephrin-B2 in Cardiovascular Development. Mol. Cell *4*, 403–414.

43. Gilbert, S.F. (2000). Regeneration.

44. Ginsburg, M., Snow, M.H., and McLaren, A. (1990). Primordial germ cells in the mouse embryo during gastrulation. Development *110*, 521–528.

45. Glick, D., Barth, S., and Macleod, K.F. (2010). Autophagy: cellular and molecular mechanisms. J. Pathol. *221*, 3–12.

46. Gurtner, G.C., Werner, S., Barrandon, Y., and Longaker, M.T. (2008). Wound repair and regeneration. Nature *453*, 314–321.

47. Gwon, A. (2006). Lens Regeneration in Mammals: A Review. Surv. Ophthalmol. *51*, 51–62.

48. Hacein-Bey-Abina, S., von Kalle, C., Schmidt, M., Le Deist, F., Wulffraat, N., McIntyre, E., Radford, I., Villeval, J.-L., Fraser, C.C., Cavazzana-Calvo, M., et al. (2003). A serious adverse event after successful gene therapy for X-linked severe combined immunodeficiency. N. Engl. J. Med. *348*, 255–256.

49. Hacein-Bey-Abina, S., Garrigue, A., Wang, G.P., Soulier, J., Lim, A., Morillon, E., Clappier, E., Caccavelli, L., Delabesse, E., Beldjord, K., et al. (2008). Insertional oncogenesis in 4 patients after retrovirus-mediated gene therapy of SCID-X1. J. Clin. Invest. *118*, 3132–3142.

50. Hamada, K., Oike, Y., Ito, Y., Maekawa, H., Miyata, K., Shimomura, T., and Suda, T. (2003). Distinct Roles of Ephrin-B2 Forward and EphB4 Reverse Signaling in Endothelial Cells. Arterioscler. Thromb. Vasc. Biol. *23*, 190–197.

51. Herzog, Y., Guttmann-Raviv, N., and Neufeld, G. (2005). Segregation of arterial and venous markers in subpopulations of blood islands before vessel formation. Dev. Dyn. *232*, 1047–1055.

52. Hochedlinger, K., and Jaenisch, R. (2006). Nuclear reprogramming and pluripotency. Nature *441*, 1061–1067.

53. Homma, K., Sone, M., Taura, D., Yamahara, K., Suzuki, Y., Takahashi, K., Sonoyama, T., Inuzuka, M., Fukunaga, Y., Tamura, N., et al. (2010). Sirt1 plays an important role in mediating greater functionality of human ES/iPS-derived vascular endothelial cells. Atherosclerosis *212*, 42–47.

54. Horner, V.L., and Wolfner, M.F. (2008). Mechanical stimulation by osmotic and hydrostatic pressure activates Drosophila oocytes in vitro in a calcium-dependent manner. Dev. Biol. *316*, 100–109.

55. Hristov, M., Erl, W., and Weber, P.C. (2003). Endothelial Progenitor Cells Mobilization, Differentiation, and Homing. Arterioscler. Thromb. Vasc. Biol. *23*, 1185–1189.

56. Ieda, M., Fu, J.-D., Delgado-Olguin, P., Vedantham, V., Hayashi, Y., Bruneau, B.G., and Srivastava, D. (2010). Direct Reprogramming of Fibroblasts into Functional Cardiomyocytes by Defined Factors. Cell *142*, 375–386.

57. Imamura, M., Okuno, H., Tomioka, I., Kawamura, Y., Lin, Z.Y.-C., Nakajima, R., Akamatsu, W., Okano, H.J., Matsuzaki, Y., Sasaki, E., et al. (2012). Derivation of induced pluripotent stem cells by retroviral gene transduction in mammalian species. Methods Mol. Biol. Clifton NJ *925*, 21–48.

58. Jopling, C., Sleep, E., Raya, M., Martí, M., Raya, A., and Belmonte, J.C.I. (2010). Zebrafish heart regeneration occurs by cardiomyocyte dedifferentiation and proliferation. Nature *464*, 606–609.

59. Jopling, C., Boue, S., and Belmonte, J.C.I. (2011). Dedifferentiation, transdifferentiation and reprogramming: three routes to regeneration. Nat. Rev. Mol. Cell Biol. *12*, 79–89.

60. Jw, C., Gl, C., Mp, D., Tl, M., and Jt, A. (1985). Lysosomal membrane glycoproteins: properties of LAMP-1 and LAMP-2. Biochem. Soc. Symp. *51*, 97–112.

61. Khan, R., and Sheppard, R. (2006). Fibrosis in heart disease: understanding the role of transforming growth factor-β1 in cardiomyopathy, valvular disease and arrhythmia. Immunology *118*, 10–24.

62. Kim, W.-S., and Stocum, D.L. (1986). Retinoic acid modifies positional memory in the anteroposterior axis of regenerating axolotl limbs. Dev. Biol. *114*, 170–179.

63. King, R.S., and Newmark, P.A. (2012). The cell biology of regeneration. J. Cell Biol. *196*, 553–562.

64. Kleinman, H.K., and Martin, G.R. (2005). Matrigel: Basement membrane matrix with biological activity. Semin. Cancer Biol. *15*, 378–386.

65. Knecht, A.K., and Bronner-Fraser, M. (2002). Induction of the neural crest: a multigene process. Nat. Rev. Genet. *3*, 453–461.

66. Kubo, A., Shinozaki, K., Shannon, J.M., Kouskoff, V., Kennedy, M., Woo, S., Fehling, H.J., and Keller, G. (2004). Development of definitive endoderm from embryonic stem cells in culture. Development *131*, 1651–1662.

67. Kurian, L., Sancho-Martinez, I., Nivet, E., Aguirre, A., Moon, K., Pendaries, C., Volle-Challier, C., Bono, F., Herbert, J.-M., Pulecio, J., et al. (2013). Conversion of human fibroblasts to angioblast-like progenitor cells. Nat. Methods *10*, 77–83.

68. Lacaud, G., Keller, G., and Kouskoff, V. (2004). Tracking Mesoderm Formation and Specification to the Hemangioblast in Vitro. Trends Cardiovasc. Med. *14*, 314–317.

69. Lambeng, N., Wallez, Y., Rampon, C., Cand, F., Christé, G., Gulino-Debrac, D., Vilgrain, I., and Huber, P. (2005). Vascular Endothelial–Cadherin Tyrosine Phosphorylation in Angiogenic and Quiescent Adult Tissues. Circ. Res. *96*, 384–391.

70. Lamouille, S., Mallet, C., Feige, J.-J., and Bailly, S. (2002). Activin receptor–like kinase 1 is implicated in the maturation phase of angiogenesis. Blood *100*, 4495–4501.

71. Lampugnani, M.G., Zanetti, A., Corada, M., Takahashi, T., Balconi, G., Breviario, F., Orsenigo, F., Cattelino, A., Kemler, R., Daniel, T.O., et al. (2003). Contact inhibition of VEGF-induced proliferation requires vascular endothelial cadherin, β-catenin, and the phosphatase DEP-1/CD148. J. Cell Biol. *161*, 793–804.

72. Lee, M.-O., Moon, S.H., Jeong, H.-C., Yi, J.-Y., Lee, T.-H., Shim, S.H., Rhee, Y.-H., Lee, S.-H., Oh, S.-J., Lee, M.-Y., et al. (2013). Inhibition of pluripotent stem cell-derived teratoma formation by small molecules. Proc. Natl. Acad. Sci. U. S. A. *110*, E3281–E3290.

73. Lepilina, A., Coon, A.N., Kikuchi, K., Holdway, J.E., Roberts, R.W., Burns, C.G., and Poss, K.D. (2006). A Dynamic Epicardial Injury Response Supports Progenitor Cell Activity during Zebrafish Heart Regeneration. Cell *127*, 607–619.

74. Lerman, A., and Zeiher, A.M. (2005). Endothelial Function Cardiac Events. Circulation *111*, 363–368.

75. Li, Z., Modlich, U., and Baum, C. (2004). Safety and efficacy in retrovirally modified haematopoietic cell therapy. Best Pract. Res. Clin. Haematol. *17*, 493–503.

76. Li, Z., Hu, S., Ghosh, Z., Han, Z., and Wu, J.C. (2011). Functional characterization and expression profiling of human induced pluripotent stem cell- and embryonic stem cell-derived endothelial cells. Stem Cells Dev. *20*, 1701–1710.

77. Lin, M.-T., Yen, M.-L., Lin, C.-Y., and Kuo, M.-L. (2003). Inhibition of Vascular Endothelial Growth Factor-Induced Angiogenesis by Resveratrol through Interruption of Src-Dependent Vascular Endothelial Cadherin Tyrosine Phosphorylation. Mol. Pharmacol. *64*, 1029–1036.

78. Maki, N., Martinson, J., Nishimura, O., Tarui, H., Meller, J., Tsonis, P.A., and Agata, K. (2010). Expression profiles during dedifferentiation in newt lens regeneration revealed by expressed sequence tags. Mol. Vis. *16*, 72–78.

79. Mammoto, T., and Ingber, D.E. (2010). Mechanical control of tissue and organ. Development *137*, 1407–1420.

80. Marcelo, K.L., Goldie, L.C., and Hirschi, K.K. (2013). Regulation of Endothelial Cell Differentiation and Specification. Circ. Res. *112*, 1272–1287.

81. Martin, B.L., and Kimelman, D. (2010). Brachyury establishes the embryonic mesodermal progenitor niche. Genes Dev. *24*, 2778–2783.

82. Masui, S., Nakatake, Y., Toyooka, Y., Shimosato, D., Yagi, R., Takahashi, K., Okochi, H., Okuda, A., Matoba, R., Sharov, A.A., et al. (2007). Pluripotency governed by Sox2 via regulation of Oct3/4 expression in mouse embryonic stem cells. Nat. Cell Biol. *9*, 625–635.

83. McGrath, K.E., Koniski, A.D., Maltby, K.M., McGann, J.K., and Palis, J. (1999). Embryonic Expression and Function of the Chemokine SDF-1 and Its Receptor, CXCR4. Dev. Biol. *213*, 442–456.

84. McLeod, D.S., Hasegawa, T., Prow, T., Merges, C., and Lutty, G. (2006). The Initial Fetal Human Retinal Vasculature Develops by Vasculogenesis. Dev. Dyn. *235*, 3336–3347.

85. Menendez, J.A., Vellon, L., Oliveras-Ferraros, C., Cufí, S., and Vazquez-Martin, A. (2011). mTOR-regulated senescence and autophagy during reprogramming of somatic cells to pluripotency: A roadmap from energy metabolism to stem cell renewal and aging. Cell Cycle *10*, 3658–3677.

86. Miller, R.J., Rostene, W., Apartis, E., Banisadr, G., Biber, K., Milligan, E.D., White, F.A., and Zhang, J. (2008). Chemokine Action in the Nervous System. J. Neurosci. Off. J. Soc. Neurosci. *28*, 11792–11795.

87. Monaghan, J.R., Athippozhy, A., Seifert, A.W., Putta, S., Stromberg, A.J., Maden, M., Gardiner, D.M., and Voss, S.R. (2012). Gene expression patterns specific to the regenerating limb of the Mexican axolotl. Biol. Open BIO20121594.

88. Naldini, L., Blömer, U., Gallay, P., Ory, D., Mulligan, R., Gage, F.H., Verma, I.M., and Trono, D. (1996). In Vivo Gene Delivery and Stable Transduction of Nondividing Cells by a Lentiviral Vector. Science *272*, 263–267.

89. Neil D. Theise, R.S. (1999). The Canals of Hering and hepatic stem cells in humans. Hepatol. Baltim. Md *30*, 1425–1433.

90. Nethercott, H.E., Brick, D.J., and Schwartz, P.H. (2011). Derivation of induced pluripotent stem cells by lentiviral transduction. Methods Mol. Biol. Clifton NJ *767*, 67–85.

91. Nichols, J., Zevnik, B., Anastassiadis, K., Niwa, H., Klewe-Nebenius, D., Chambers, I., Schöler, H., and Smith, A. (1998). Formation of pluripotent stem cells in the mammalian embryo depends on the POU transcription factor Oct4. Cell *95*, 379–391.

92. Niwa, H., Miyazaki, J., and Smith, A.G. (2000). Quantitative expression of Oct-3/4 defines differentiation, dedifferentiation or self-renewal of ES cells. Nat. Genet. *24*, 372–376.

93. North, T.E., Goessling, W., Peeters, M., Li, P., Ceol, C., Lord, A.M., Weber, G.J., Harris, J., Cutting, C.C., Huang, P., et al. (2009). Hematopoietic Stem Cell Development Is Dependent on Blood Flow. Cell *137*, 736–748.

94. Nourse, M.B., Halpin, D.E., Scatena, M., Mortisen, D.J., Tulloch, N.L., Hauch, K.D., Torok-Storb, B., Ratner, B.D., Pabon, L., and Murry, C.E. (2010). VEGF Induces Differentiation of Functional Endothelium From Human Embryonic Stem Cells Implications for Tissue Engineering. Arterioscler. Thromb. Vasc. Biol. *30*, 80–89.

95. Okita, K., Ichisaka, T., and Yamanaka, S. (2007). Generation of germline-competent induced pluripotent stem cells. Nature *448*, 313–317.

96. Ørn, S., Manhenke, C., Anand, I.S., Squire, I., Nagel, E., Edvardsen, T., and Dickstein, K. (2007). Effect of Left Ventricular Scar Size, Location, and Transmurality on Left Ventricular Remodeling With Healed Myocardial Infarction. Am. J. Cardiol. *99*, 1109–1114.

97. Pan, G.J., Chang, Z.Y., Schöler, H.R., and Pei, D. (2002). Stem cell pluripotency and transcription factor Oct4. Cell Res. *12*, 321–329.

98. Park, C., Kim, T.M., and Malik, A.B. (2013). Transcriptional Regulation of Endothelial Cell and Vascular Development. Circ. Res. *112*, 1380–1400.

99. dela Paz, N.G., and D'Amore, P.A. (2009). Arterial versus venous endothelial cells. Cell Tissue Res. *335*, 5–16.

100. Pennock, R., Bray, E., Pryor, P., James, S., McKeegan, P., Sturmey, R., and Genever, P. (2015a). Human cell dedifferentiation in mesenchymal condensates through controlled autophagy. Sci. Rep. *5*, 13113.

101. Persons, D.A. (2010). Lentiviral Vector Gene Therapy: Effective and Safe? Mol. Ther. *18*, 861–862.

102. Pevny, L.H., Sockanathan, S., Placzek, M., and Lovell-Badge, R. (1998). A role for SOX1 in neural determination. Dev. Camb. Engl. *125*, 1967–1978.

103. Podgrabinska, S., Braun, P., Velasco, P., Kloos, B., Pepper, M.S., Jackson, D.G., and Skobe, M. (2002). Molecular characterization of lymphatic endothelial cells. Proc. Natl. Acad. Sci. *99*, 16069–16074.

104. Poh, Y.-C., Chen, J., Hong, Y., Yi, H., Zhang, S., Chen, J., Wu, D.C., Wang, L., Jia, Q., Singh, R., et al. (2014). Generation of organized germ layers from a single mouse embryonic stem cell. Nat. Commun. *5*.

105. Poss, K.D., Wilson, L.G., and Keating, M.T. (2002). Heart Regeneration in Zebrafish. Science *298*, 2188–2190.

106. Rajendran, P., Rengarajan, T., Thangavel, J., Nishigaki, Y., Sakthisekaran, D., Sethi, G., and Nishigaki, I. (2013). The Vascular Endothelium and Human Diseases. Int. J. Biol. Sci. *9*, 1057–1069.

107. Rathjen, J., Lake, J.A., Bettess, M.D., Washington, J.M., Chapman, G., and Rathjen, P.D. (1999). Formation of a primitive ectoderm like cell population, EPL cells, from ES cells in response to biologically derived factors. J. Cell Sci. *112*, 601–612.

108. Reddien, P.W., and Sánchez Alvarado, A. (2004). Fundamentals of planarian regeneration. Annu. Rev. Cell Dev. Biol. *20*, 725–757.

109. Reddien, P.W., Bermange, A.L., Murfitt, K.J., Jennings, J.R., and Sánchez Alvarado, A. (2005). Identification of Genes Needed for Regeneration, Stem Cell Function, and Tissue Homeostasis by Systematic Gene Perturbation in Planaria. Dev. Cell *8*, 635–649.

110. Reed, D.M., Foldes, G., Harding, S.E., and Mitchell, J.A. (2013). Stem cell-derived endothelial cells for cardiovascular disease: a therapeutic perspective. Br. J. Clin. Pharmacol. *75*, 897–906.

111. Rettig, M.P., Ansstas, G., and DiPersio, J.F. (2012). Mobilization of hematopoietic stem and progenitor cells using inhibitors of CXCR4 and VLA-4. Leukemia *26*, 34–53.

112. Saunders, R.L., and Hammer, D.A. (2010). Assembly of Human Umbilical Vein Endothelial Cells on Compliant Hydrogels. Cell. Mol. Bioeng. *3*, 60–67.

113. Sayed, N., Wong, W.T., Ospino, F., Meng, S., Lee, J., Jha, A., Dexheimer, P., Aronow, B.J., and Cooke, J.P. (2014). Transdifferentiation of Human Fibroblasts to Endothelial Cells: Role of Innate Immunity. Circulation CIRCULATIONAHA.113.007394.

114. Settembre, C., Di Malta, C., Polito, V.A., Arencibia, M.G., Vetrini, F., Erdin, S., Erdin, S.U., Huynh, T., Medina, D., Colella, P., et al. (2011). TFEB Links Autophagy to Lysosomal Biogenesis. Science *332*, 1429–1433.

115. Shalaby, F., Rossant, J., Yamaguchi, T.P., Gertsenstein, M., Wu, X.F., Breitman, M.L., and Schuh, A.C. (1995). Failure of blood-island formation and vasculogenesis in Flk-1-deficient mice. Nature *376*, 62–66.

116. Smith, J.C., Price, B.M.J., Green, J.B.A., Weigel, D., and Herrmann, B.G. (1991). Expression of a xenopus homolog of Brachyury (T) is an immediate-early response to mesoderm induction. Cell *67*, 79–87.

117. Soda, Y., Marumoto, T., Friedmann-Morvinski, D., Soda, M., Liu, F., Michiue, H., Pastorino, S., Yang, M., Hoffman, R.M., Kesari, S., et al. (2011). Transdifferentiation of glioblastoma cells into vascular endothelial cells. Proc. Natl. Acad. Sci. *108*, 4274–4280.

118. Sugiyama, T., Kohara, H., Noda, M., and Nagasawa, T. (2006). Maintenance of the Hematopoietic Stem Cell Pool by CXCL12-CXCR4 Chemokine Signaling in Bone Marrow Stromal Cell Niches. Immunity *25*, 977–988.

119. Tadeu, A.M.B., Lin, S., Hou, L., Chung, L., Zhong, M., Zhao, H., and Horsley, V. (2015). Transcriptional Profiling of Ectoderm Specification to Keratinocyte Fate in Human Embryonic Stem Cells. PLoS ONE *10*, e0122493.

120. Takahashi, K., and Yamanaka, S. (2006). Induction of Pluripotent Stem Cells from Mouse Embryonic and Adult Fibroblast Cultures by Defined Factors. Cell *126*, 663–676.

121. Takahashi, K., Tanabe, K., Ohnuki, M., Narita, M., Ichisaka, T., Tomoda, K., and Yamanaka, S. (2007). Induction of pluripotent stem cells from adult human fibroblasts by defined factors. Cell *131*, 861–872.

122. Takenaga, M., Fukumoto, M., and Hori, Y. (2007). Regulated Nodal signaling promotes differentiation of the definitive endoderm and mesoderm from ES cells. J. Cell Sci. *120*, 2078–2090.

123. Takeuchi, T. (2014). Regulation of cardiomyocyte proliferation during development and regeneration. Dev. Growth Differ. *56*, 402–409.

124. Tanaka, E.M. (2003). Regeneration: If They Can Do It, Why Can't We? Cell *113*, 559–562.

125. Thomson, J.A., Itskovitz-Eldor, J., Shapiro, S.S., Waknitz, M.A., Swiergiel, J.J., Marshall, V.S., and Jones, J.M. (1998). Embryonic Stem Cell Lines Derived from Human Blastocysts. Science *282*, 1145–1147.

126. Thomson, M., Liu, S.J., Zou, L.-N., Smith, Z., Meissner, A., and Ramanathan, S. (2011). Pluripotency Factors in Embryonic Stem Cells Regulate Differentiation into Germ Layers. Cell *145*, 875–889.

127. Tsonis, P.A. (1996). Limb Regeneration (Cambridge University Press).

128. Tsonis, P.A., Madhavan, M., Tancous, E.E., and Del Rio-Tsonis, K. (2004). A newt's eye view of lens regeneration. Int. J. Dev. Biol. *48*, 975–980.

129. Urness, L.D., Sorensen, L.K., and Li, D.Y. (2000). Arteriovenous malformations in mice lacking activin receptor-like kinase-1. Nat. Genet. *26*, 328–331.

130. Valdimarsdottir, G., Goumans, M.-J., Rosendahl, A., Brugman, M., Itoh, S., Lebrin, F., Sideras, P., and Dijke, P. ten (2002). Stimulation of Id1 Expression by Bone Morphogenetic Protein Is Sufficient and Necessary for Bone Morphogenetic Protein–Induced Activation of Endothelial Cells. Circulation *106*, 2263–2270.

131. Varga, M., Sass, M., Papp, D., Takács-Vellai, K., Kobolak, J., Dinnyés, A., Klionsky, D.J., and Vellai, T. (2014). Autophagy is required for zebrafish caudal fin regeneration. Cell Death Differ. *21*, 547–556.

132. Varum, S., Rodrigues, A.S., Moura, M.B., Momcilovic, O., Easley, C.A., Ramalho-Santos, J., Van Houten, B., and Schatten, G. (2011). Energy Metabolism in Human Pluripotent Stem Cells and Their Differentiated Counterparts. PLoS ONE *6*, e20914.

133. van de Ven, C., Collins, D., Bradley, M.B., Morris, E., and Cairo, M.S. (2007). The potential of umbilical cord blood multipotent stem cells for nonhematopoietic tissue and cell regeneration. Exp. Hematol. *35*, 1753–1765.

134. Verhamme, P., and Hoylaerts, M.F. (2006). The pivotal role of the endothelium in haemostasis and thrombosis. Acta Clin. Belg. *61*, 213–219.

135. Verhoeyen, E., Costa, C., and Cosset, F.-L. (2009). Lentiviral vector gene transfer into human T cells. Methods Mol. Biol. Clifton NJ *506*, 97–114.

136. Vestweber, D. (2008). VE-cadherin: the major endothelial adhesion molecule controlling cellular junctions and blood vessel formation. Arterioscler. Thromb. Vasc. Biol. *28*, 223–232.

137. Voyta, J.C., Via, D.P., Butterfield, C.E., and Zetter, B.R. (1984). Identification and isolation of endothelial cells based on their increased uptake of acetylated-low density lipoprotein. J. Cell Biol. *99*, 2034–2040.

138. Wang, H.U., and Anderson, D.J. (1997). Eph Family Transmembrane Ligands Can Mediate Repulsive Guidance of Trunk Neural Crest Migration and Motor Axon Outgrowth. Neuron *18*, 383–396.

139. Wang, A., Tang, Z., Park, I.-H., Zhu, Y., Patel, S., Daley, G.Q., and Li, S. (2011). Induced pluripotent stem cells for neural tissue engineering. Biomaterials *32*, 5023–5032.

140. Wang, H.U., Chen, Z.-F., and Anderson, D.J. (1998). Molecular Distinction and Angiogenic Interaction between Embryonic Arteries and Veins Revealed by ephrin-B2 and Its Receptor Eph-B4. Cell *93*, 741–753.

141. Wang, M., Su, Y., Sun, H., Wang, T., Yan, G., Ran, X., Wang, F., Cheng, T., and Zou, Z. (2010). Induced endothelial differentiation of cells from a murine embryonic mesenchymal cell line C3H/10T1/2 by angiogenic factors in vitro. Differentiation *79*, 21–30.

142. Wang, N., Zhang, R., Wang, S.-J., Zhang, C.-L., Mao, L.-B., Zhuang, C.-Y., Tang, Y.-Y., Luo, X.-G., Zhou, H., and Zhang, T.-C. (2013). Vascular endothelial growth factor stimulates endothelial differentiation from mesenchymal stem cells via Rho/myocardin-related transcription factor-A signaling pathway. Int. J. Biochem. Cell Biol. *45*, 1447–1456.

143. Watson, A.J. (1992). The cell biology of blastocyst development. Mol. Reprod. Dev. *33*, 492–504.

144. Wei, X., Yang, X., Han, Z., Qu, F., Shao, L., and Shi, Y. (2013). Mesenchymal stem cells: a new trend for cell therapy. Acta Pharmacol. Sin. *34*, 747–754.

145. Winnier, G., Blessing, M., Labosky, P.A., and Hogan, B.L. (1995). Bone morphogenetic protein-4 is required for mesoderm formation and patterning in the mouse. Genes Dev. *9*, 2105–2116.

146. Xiong, J.-W. (2008). Molecular and Developmental Biology of the Hemangioblast. Dev. Dyn. Off. Publ. Am. Assoc. Anat. *237*, 1218–1231.

147. Xu, C., Police, S., Rao, N., and Carpenter, M.K. (2002). Characterization and Enrichment of Cardiomyocytes Derived From Human Embryonic Stem Cells. Circ. Res. *91*, 501–508.

148. Yamada, Y., Warren, A.J., Dobson, C., Forster, A., Pannell, R., and Rabbitts, T.H. (1998). The T cell leukemia LIM protein Lmo2 is necessary for adult mouse hematopoiesis. Proc. Natl. Acad. Sci. U. S. A. *95*, 3890–3895.

149. Young, H.E., and Black, A.C. (2004). Adult stem cells. Anat. Rec. *276A*, 75–102.

150. Yu, J., Vodyanik, M.A., Smuga-Otto, K., Antosiewicz-Bourget, J., Frane, J.L., Tian, S., Nie, J., Jonsdottir, G.A., Ruotti, V., Stewart, R., et al. (2007). Induced Pluripotent Stem Cell Lines Derived from Human Somatic Cells. Science *318*, 1917–1920.

151. Zhang, P., Li, J., Tan, Z., Wang, C., Liu, T., Chen, L., Yong, J., Jiang, W., Sun, X., Du, L., et al. (2008). Short-term BMP-4 treatment initiates mesoderm induction in human embryonic stem cells. Blood *111*, 1933–1941.

152. Zhang, Y., Li, T.-S., Lee, S.-T., Wawrowsky, K.A., Cheng, K., Galang, G., Malliaras, K., Abraham, M.R., Wang, C., and Marbán, E. (2010). Dedifferentiation and Proliferation of Mammalian Cardiomyocytes. PLoS ONE *5*, e12559.

153. Zhang, Y., Mignone, J., and MacLellan, W.R. (2015). Cardiac Regeneration and Stem Cells. Physiol. Rev. *95*, 1189–1204.

154. Zorn, A.M., and Wells, J.M. (2009). Vertebrate Endoderm Development and Organ Formation. Annu. Rev. Cell Dev. Biol. *25*, 221–251.

155. Zwi, L., Caspi, O., Arbel, G., Huber, I., Gepstein, A., Park, I.-H., and Gepstein, L. (2009). Cardiomyocyte Differentiation of Human Induced Pluripotent Stem Cells. Circulation *120*, 1513–1523.